

## Polychromatic Solitary Waves in a Periodic and Nonlinear Maxwell System\*

Dmitry E. Pelinovsky<sup>†</sup>, Gideon Simpson<sup>‡</sup>, and Michael I. Weinstein<sup>§</sup>

**Abstract.** We consider the one-dimensional Maxwell equations with low contrast periodic linear refractive index and weak Kerr nonlinearity. In this context, wave packet initial conditions with a single carrier frequency excite infinitely many resonances. On large but finite time-scales, the coupled evolution of backward and forward waves is governed by nonlocal equations of resonant nonlinear geometrical optics. For the special class of solutions which are periodic in the fast phase, these equations are equivalent to an infinite system of nonlinear coupled mode equations, the so-called *extended nonlinear coupled mode equations*, or xNLCME. Numerical studies support the existence of long-lived spatially localized coherent structures, featuring a slowly varying envelope and a train of *carrier shocks*. In this paper we explore, by analytical, asymptotic, and numerical methods, the existence and properties of spatially localized structures of the xNLCME system for the case where the refractive index profile consists of a periodic array of Dirac delta functions. We consider, in particular, the limit of small amplitude solutions with frequencies near a spectral band edge. In this case, stationary xNLCME is well approximated by an infinite system of coupled, stationary, nonlinear Schrödinger (NLS) equations, the *extended nonlinear Schrödinger system*, xNLS. We embed xNLS in a one-parameter family of equations, xNLS<sup>ε</sup>, which interpolates between infinitely many decoupled NLS equations ( $\epsilon = 0$ ) and xNLS ( $\epsilon = 1$ ). Using bifurcation methods we show existence of solutions for a range of  $\epsilon \in (-\epsilon_0, \epsilon_0)$  and, by a numerical continuation method, establish the continuation of certain branches all the way to  $\epsilon = 1$ . Finally, we perform time-dependent simulations of a truncated xNLCME and find the small-amplitude near-band edge gap solitons to be robust to both numerical errors and the NLS approximation.

**Key words.** nonlinear Maxwell equations, coupled mode equations, nonlinear Schrödinger equations, existence of solitons

**AMS subject classifications.** 78A25, 37K40, 65L07

**DOI.** 10.1137/110837899

**1. Introduction and overview.** Nonlinear waves in periodic structures have been a subject of great interest for many years. Early interest arose from the possibility of balancing the *band dispersion* of the periodic structure with the nonlinearity to form soliton-like structures; see, for example, [6, 12] and references cited therein. While such a heterogeneous medium possesses the same soliton-producing ingredients of dispersion and nonlinearity found in the well-known

\*Received by the editors June 20, 2011; accepted for publication (in revised form) by A. Scheel January 5, 2012; published electronically March 22, 2012.

<http://www.siam.org/journals/siads/11-1/83789.html>

<sup>†</sup>Department of Mathematics and Statistics, McMaster University, Hamilton L8S 4K1, ON, Canada ([dmpeli@math.mcmaster.ca](mailto:dmpeli@math.mcmaster.ca)). The work of this author was supported by NSERC.

<sup>‡</sup>School of Mathematics, University of Minnesota, Minneapolis, MN 55455 ([gsimpson@umn.edu](mailto:gsimpson@umn.edu)). The work of this author was supported in part by NSERC and was completed at the University of Minnesota while the author was supported by NSF PIRE grant OISE-0967140 and DOE grant DE-SC0002085.

<sup>§</sup>Department of Applied Physics and Applied Mathematics, Columbia University, New York, NY 10027 ([miw2103@columbia.edu](mailto:miw2103@columbia.edu)). The work of this author was supported in part by NSF grants DMS-07-07850 and DMS-10-08855.

Korteweg–de Vries (KdV) and nonlinear Schrödinger (NLS) equations, which govern nonlinear dispersive waves in spatially homogeneous media, periodic variations of the medium introduce additional possibilities. Indeed, changing the periodicity and material contrasts of the medium may permit tuning of the dispersive properties; e.g., the length scale on which a soliton can form may be altered. Thus, nonlinear and periodic structures are natural candidates for device design and applications. An example is the formation of centimeter-scale *gap solitons* in periodic optical fiber gratings. Such states have been shown to propagate at a fraction of the speed of light and have been proposed in schemes for optical storage and buffering; see, for example, [13].

In the simplest setting, nonlinear electromagnetic waves in a one-dimensional periodic structure are governed by a nonlinear Maxwell equation:

$$(1.1) \quad \partial_t^2 (n^2(z)E + \chi E^3) = \partial_z^2 E.$$

Here,  $\chi > 0$  is the Kerr nonlinearity coefficient [3]. We assume a low-contrast, periodic refractive index profile,  $n(z)$ , with mean  $n_0$ , given by

$$(1.2) \quad n(z) = n_0 + \epsilon N(z), \quad n_0 > 0, \quad N(z) = N(z + 2\pi), \quad 0 < \epsilon \ll 1,$$

where  $n(z)$  is real-valued and no energy dissipation has been included. The periodic part of the refractive index,  $N(z)$ , can be expanded in the Fourier series

$$(1.3) \quad N(z) = \sum_{p \in \mathbb{Z}} N_p e^{ipz}, \quad N_{-p} = \bar{N}_p, \quad p \in \mathbb{Z}.$$

To ensure a nontrivial Bragg resonance, let us assume  $N_2 \neq 0$ . Then strong dispersion is excited by wave packet-type initial conditions consisting of a slowly modulated plane wave of a single frequency, chosen to be in (Bragg) resonance with the periodicity of the medium:

$$(1.4) \quad E(z, t = 0) = \epsilon^{\frac{1}{2}} [E_1^+(\epsilon z, 0)e^{iz} + E_1^-(\epsilon z, 0)e^{-iz} + \text{c.c.}],$$

where  $E_1^\pm(Z, 0)$  are spatially localized in  $Z = \epsilon z$  and c.c. denotes the complex conjugate of the preceding expression. This resonance strongly couples backward and forward propagating waves. In the choice of initial condition (1.4), dispersive effects which are set by the medium contrast, of size  $\mathcal{O}(\epsilon)$ , have been balanced with nonlinear effects by choosing the amplitude to be of size  $\mathcal{O}(\epsilon^{\frac{1}{2}})$ .

Suppose we make a formal multiple scale expansion based on the ansatz:

$$(1.5) \quad E(z, t) = \epsilon^{\frac{1}{2}} [E_1^+(Z, T)e^{i(z-v_g t)} + E_1^-(Z, T)e^{-i(z+v_g t)} + \text{c.c.} + \mathcal{O}(\epsilon)],$$

$$T = \epsilon t, \quad Z = \epsilon z, \quad v_g \equiv \frac{1}{n_0}.$$

Then if we account only for the principal harmonics, we arrive at the nonlinear coupled mode equations (NLCME) for  $E_1^\pm(Z, T)$ :

$$(1.6a) \quad \partial_T E_1^+ + v_g \partial_Z E_1^+ = iv_g^2 (N_0 E_1^+ + N_2 E_1^-) + i\Gamma (|E_1^+|^2 + 2|E_1^-|^2) E_1^+,$$

$$(1.6b) \quad \partial_T E_1^- - v_g \partial_Z E_1^- = iv_g^2 (\bar{N}_2 E_1^+ + N_0 E_1^-) + i\Gamma (|E_1^-|^2 + 2|E_1^+|^2) E_1^-,$$

where  $\Gamma \equiv 3\chi/(2n_0^3)$ .  $E_1^\pm$  denote slowly varying forward and backward wave amplitudes; for details see [6] and references cited therein.

NLCME has been rigorously derived as a leading order model in numerous contexts. For one-dimensional propagation of electromagnetic waves in nonlinear and periodic media, it was rigorously derived from the anharmonic Maxwell–Lorentz model in [14]. Derivations from the Klein–Fock as well as the Gross–Pitaevskii equations have also been obtained; see [18, 19, 15, 16]. Explicit localized stationary solutions, called *gap solitons*, for NLCME are given in [1, 4]. The linear stability of the gap solitons was studied in [5], and a linear, multidimensional, analogue of NLCME was studied in [2].

However, NLCME is *not* the correct mathematical description of weakly nonlinear and weakly dispersive waves in the nonlinear and periodic Maxwell equation (1.1), with index of refraction given by (1.2). The deficiency of the NLCME system, (1.6), stems from the unperturbed ( $\epsilon = 0$ ) equation being the *nondispersive* one-dimensional wave equation. Due to nonlinearity, a single frequency initial condition (1.4) excites infinitely many resonances, since  $e^{im(z \pm t/n_0)}$ ,  $m \in \mathbb{Z}$ , all lie in the kernel of the unperturbed operator,  $n_0^2 \partial_t^2 - \partial_z^2$ . In contrast, other models, such as the aforementioned anharmonic Maxwell–Lorentz system and the Gross–Pitaevskii equation, remain dispersive in the  $\epsilon = 0$  limit; this precludes infinitely many resonant modes.

In [21], nonlocal equations derived from nonlinear geometrical optics and an equivalent system of infinitely many coupled PDEs, which take into account the infinitely many resonances, were systematically studied. One begins with the general weakly nonlinear ansatz,

$$(1.7) \quad E(z, t) = \epsilon^{\frac{1}{2}} [E^+(Z, T, z - v_g t) + E^-(Z, T, z + v_g t) + \mathcal{O}(\epsilon)],$$

which need not be nearly monochromatic. A necessary condition for the error term in (1.7) to be of order  $\epsilon$  on the time interval  $0 \leq t \leq \mathcal{O}(\epsilon^{-1})$  is that the forward and backward wave components,  $E^\pm(Z, T, \phi_\pm)$ ,  $\phi_\pm = z \mp v_g t$ , satisfy the system of nonlocal evolution equations:

$$(1.8a) \quad \begin{aligned} (\partial_T + v_g \partial_Z + v_g^2 N_0 \partial_\phi) E^+ &= v_g^2 \partial_\phi \left[ \frac{1}{2\pi} \int_{-\pi}^\pi N(\phi + \theta) E^-(Z, T, \phi + 2\theta) d\theta \right] \\ &+ \frac{\Gamma}{3} \partial_\phi \left[ (E^+)^3 + 3 \left( \frac{1}{2\pi} \int_{-\pi}^\pi |E^-(Z, T, \theta)|^2 d\theta \right) E^+ \right], \end{aligned}$$

$$(1.8b) \quad \begin{aligned} (\partial_T - v_g \partial_Z - v_g^2 N_0 \partial_\phi) E^- &= -v_g^2 \partial_\phi \left[ \frac{1}{2\pi} \int_{-\pi}^\pi N(\phi - \theta) E^+(Z, T, \phi - 2\theta) d\theta \right] \\ &- \frac{\Gamma}{3} \partial_\phi \left[ (E^-)^3 + 3 \left( \frac{1}{2\pi} \int_{-\pi}^\pi |E^+(Z, T, \theta)|^2 d\theta \right) E^- \right]. \end{aligned}$$

While we have omitted the  $\pm$  subscripts on  $\partial_\phi$  derivatives for the sake of brevity, the reader should note that in recovering the primitive field, as in (1.7),  $E^+$  must be evaluated at  $\phi_+$  and  $E^-$  must be evaluated at  $\phi_-$ .  $E^\pm(Z, T, \phi_\pm)$  are assumed to be  $2\pi$ -periodic in their  $\phi_\pm$  arguments. A similar but more general system of integro-differential equations was obtained in [21]. In that work, the authors set  $N_0 = 0$  and  $v_g = 1$ .

If we expand  $E^\pm(Z, T, \phi)$  in a Fourier series with respect to the phase variable  $\phi$ ,

$$(1.9) \quad E^\pm(Z, T, \phi) = \sum_{p \in \mathbb{Z}} E_p^\pm(Z, T) e^{\pm ip\phi},$$

the nonlocal system (1.8) may be re-expressed as a system of *infinitely* many nonlinear coupled mode (differential) equations for the Fourier mode coefficients, indexed by  $p \in \mathbb{Z}$ :

$$(1.10a) \quad \begin{aligned} \partial_T E_p^+ + v_g \partial_Z E_p^+ &= ipv_g^2 (N_0 E_p^+ + N_{2p} E_p^-) \\ &+ ip \frac{\Gamma}{3} \left[ \sum_{q,r \in \mathbb{Z}} E_q^+ E_r^+ \bar{E}_{q+r-p}^+ + 3 \left( \sum_{q \in \mathbb{Z}} |E_q^-|^2 \right) E_p^+ \right], \end{aligned}$$

$$(1.10b) \quad \begin{aligned} \partial_T E_p^- - v_g \partial_Z E_p^- &= ipv_g^2 (N_{-2p} E_p^+ + N_0 E_p^-) \\ &+ ip \frac{\Gamma}{3} \left[ \sum_{q,r \in \mathbb{Z}} E_q^- E_r^- \bar{E}_{q+r-p}^- + 3 \left( \sum_{q \in \mathbb{Z}} |E_q^+|^2 \right) E_p^- \right]. \end{aligned}$$

In [21] the infinite system of PDEs (1.10) is referred to as the *extended nonlinear coupled mode equations*, or xNLCME. Thus xNLCME is an extension of the classical NLCME (1.6), appropriate for *highly resonant* settings, such as the weakly periodic and nonlinear Maxwell model (1.1). Truncation of xNLCME to a single mode,  $E_1^\pm(Z, T)$ , yields NLCME (1.6), which, as noted earlier, has spatially localized gap soliton solutions.

Numerical simulations of the primitive nonlinear and periodic Maxwell equation (1.1) give evidence of two phenomena. First, there appear to be long-lived spatially localized coherent structures. Second, within such spatially localized structures, a train of *carrier shocks* can form. These structures appear to be well described by xNLCME [21].

The nonlinear Maxwell equation (1.1) does not incorporate any effects of chromatic dispersion which, as in the anharmonic Maxwell–Lorentz model [14], *takes higher harmonics off resonance*. However, chromatic dispersion on the length scales of many experiments is a negligible effect [11]. Moreover, there are experimentally realizable regimes in which pulses with spectral content near the zero dispersion point are propagated [17]. In these experiments, a broad band *supercontinuum* is generated. The carrier shocking mentioned above is a possible source of such broad band emission.

In this paper, we explore, by analytical, asymptotic, and numerical methods, the existence and properties of spatially localized structures of xNLCME. These coherent solutions have a full spectrum of active temporal frequencies, and we therefore refer to them as *polychromatic solitons*, to use the terminology of [22]. In that work the authors considered a truncation of xNLCME to first and third harmonics. Studying the problem numerically, they found evidence for the existence of spatially localized solutions with two basic frequencies and named them polychromatic solitons. The localized structures we study have an infinite number of discrete carrier frequencies.

We focus on the stationary, small amplitude approximation of xNLCME for a particular choice of refractive index consisting of an infinite periodic array of Dirac delta functions. In particular, we consider solutions spectrally concentrated near a band edge. In this regime, xNLCME is well approximated by an infinite system of coupled nonlinear Schrödinger equations, the *extended nonlinear Schrödinger system*, or xNLS. We embed xNLS in a one-parameter family of equations, xNLS $^\epsilon$ , which continuously interpolates between a system of infinitely many decoupled NLS equations ( $\epsilon = 0$ ) and xNLS ( $\epsilon = 1$ ). Using bifurcation methods based on the Lyapunov–Schmidt method and the implicit function theorem, we prove

the existence of solutions for a range of  $\epsilon \in (-\epsilon_0, \epsilon_0)$ . By a numerical continuation method, we establish the persistence of *certain* branches all the way to  $\epsilon = 1$  for finite truncations of  $\text{xNLS}^\epsilon$ . Finally, we perform time-dependent simulations of  $\text{xNLCME}$  and find the small amplitude near-band edge gap solitons to be robust.

*Outline of the paper.* In section 2, we present a direct derivation of  $\text{xNLCME}$  in the case of a periodic medium and show the sense in which  $\text{xNLCME}$  is an infinite dimensional Hamiltonian system. In section 3 we heuristically determine conditions on  $N(z)$  for which we may expect exponentially localized gap solitons. This motivates our study of the case where  $N(z)$  is a periodic array of delta functions.

In the small amplitude, near-band edge limit where  $\text{xNLCME}$  reduces to  $\text{xNLS}$ , we conjecture that localized stationary solutions of  $\text{xNLS}$  exist. Subject to this assumption, we prove in Theorem 3.1 that the gap soliton persists within  $\text{xNLCME}$ , in the asymptotic limit. Since the energy of  $\text{xNLS}$  is bounded below, it is natural to ask whether a ground state of  $\text{xNLS}$  can be constructed variationally. Unfortunately, standard methods do not apply due to a loss of compactness, illustrated in section 3.2.3. The existence of nontrivial critical points is an open problem.

We therefore seek to construct localized states via a continuation method. First, we embed  $\text{xNLS}$  in a one-parameter family of systems,  $\text{xNLS}^\epsilon$ , with  $\epsilon = 0$  corresponding to an infinite system of decoupled NLS equations, and  $\epsilon = 1$  corresponding to  $\text{xNLS}$ , the system of interest. In Theorem 3.2, we prove the existence of gap solitons for  $\text{xNLS}^\epsilon$  for an open interval of  $|\epsilon| < \epsilon_0$  about  $\epsilon = 0$ .

We next attempt to numerically continue  $\text{xNLS}^\epsilon$  solitons to the full interval  $[0, 1]$ . In order to implement the numerical continuation, we seek approximate critical points of the  $\text{xNLS}^\epsilon$  variational problem. To motivate this, in section 4, we replace the variational characterization of  $\text{xNLS}^\epsilon$  solitons by a finite dimensional minimization problem over families of Gaussian trial functions. We find critical points, with sign alternating amplitudes, of such finite dimensional approximations and give convincing numerical evidence that some can be continued to  $\epsilon = 1$ .

In section 5 we compute soliton solutions of truncated  $\text{xNLS}$  using information gleaned from the trial function approximations, and show that they are robust in time-dependent simulations of the truncated system. Section 6 summarizes our findings and highlights open problems.

**2. Coupled mode equations.** In section 2.1, we present a derivation of  $\text{xNLCME}$  from Maxwell equations using Fourier expansions of  $E^\pm(Z, T, \phi_\pm)$ , in the case where  $E^\pm(Z, T, \phi_\pm)$  are periodic in  $\phi_\pm$ . In section 2.2, we demonstrate that  $\text{xNLCME}$  is an infinite dimensional Hamiltonian system with two conserved quantities.

**2.1. Derivation of  $\text{xNLCME}$  in a periodically varying medium.** For simplicity and without loss of generality, we set  $n_0 = 1$  so that  $v_g \equiv 1$ . We rewrite the nonlinear Maxwell equation (1.1) with refractive index (1.2) as

$$(2.1) \quad \partial_z^2 E - \partial_t^2 E = 2\epsilon N(z) \partial_t^2 E + \epsilon^2 N(z)^2 \partial_t^2 E + \chi \partial_t^2 E^3.$$

For  $\epsilon = 0$  and  $\chi = 0$ , (2.1) simplifies to the one-dimensional wave equation with a solution given by the arbitrary superposition of right and left traveling waves,

$$(2.2) \quad E^{(0)}(z, t) = E^+(z - t) + E^-(z + t).$$

For  $\epsilon$  small, we seek  $E = E^\epsilon(z, t)$  in the form of a multiple scale expansion

$$(2.3) \quad E(z, t) = \epsilon^{\frac{1}{2}} \left( E^{(0)}(Z, T; z, t) + \epsilon E^{(1)}(Z, T; z, t) + \mathcal{O}(\epsilon^2) \right),$$

where  $Z = \epsilon z$  and  $T = \epsilon t$  are slow spatial and temporal scales. Substituting (2.3) into (2.1), we obtain at first order in  $\epsilon$

$$(2.4) \quad (\partial_z^2 - \partial_t^2) E^{(1)} = 2(\partial_t \partial_T - \partial_z \partial_Z) E^{(0)} + 2N(z) \partial_t^2 E^{(0)} + \chi \partial_t^2 \left( E^{(0)} \right)^3.$$

The right-hand-side of (2.4) generates resonant terms along the characteristics of the wave equation, leading to secular growth of the correction  $E^{(1)}$  in  $(z, t)$ . The slow evolution in  $(Z, T)$  is determined to remove these secular terms.

We begin by expanding  $E$  in a Fourier series:

$$(2.5) \quad E^\pm(Z, T; z, t) = \sum_{p \in \mathbb{Z}} E_p^\pm(Z, T) e^{\pm ip(z \mp t)}, \quad E^{(1)}(Z, T; z, t) = \sum_{p \in \mathbb{Z}} E_p^{(1)}(Z, T; t) e^{ipz}.$$

Since  $E^\pm$  are real-valued,

$$(2.6) \quad \bar{E}_p^\pm(Z, T) = E_{-p}^\pm(Z, T), \quad p \in \mathbb{Z}.$$

Substituting (2.5) into (2.4), the terms of the equation proportional to  $e^{ipz}$  are

$$\begin{aligned} (\partial_t^2 + p^2) E_p^{(1)} &= 2ip(\partial_T + \partial_Z) E_p^+ e^{-ipt} - 2ip(\partial_T - \partial_Z) E_{-p}^- e^{ipt} \\ &\quad + 2 \sum_q q^2 (N_{p-q} E_q^+ e^{-iqt} + N_{p+q} E_q^- e^{-iqt}) \\ &\quad + \chi \sum_{q,r} p^2 E_q^+ E_r^+ \bar{E}_{q+r-p}^+ e^{-ipt} + 2\chi \sum_{q,r} (p - 2q + 2r)^2 E_q^+ \bar{E}_r^+ E_{q-r-p}^- e^{i(p-2q+2r)t} \\ &\quad + \chi \sum_{q,r} (p + 2q + 2r)^2 E_q^- E_r^- \bar{E}_{-p-q-r}^+ e^{-i(p+2q+2r)t} \\ &\quad + \chi \sum_{q,r} (p - 2q - 2r)^2 E_q^+ E_r^+ \bar{E}_{p-q-r}^- e^{i(p-2q-2r)t} \\ &\quad + 2\chi \sum_{q,r} (p + 2q - 2r)^2 E_q^- \bar{E}_r^- E_{p+q-r}^+ e^{-i(p+2q-2r)t} \\ &\quad + \chi \sum_{q,r} p^2 E_q^- \bar{E}_r^- E_{-p-q+r}^- e^{ipt}, \end{aligned}$$

where all sums are taken over  $\mathbb{Z}$ . Removing the terms resonant with  $e^{-ipt}$ , we obtain

$$(2.7a) \quad \begin{aligned} (\partial_T + \partial_Z) E_p^+ &= ip(N_0 E_p^+ + N_{2p} E_p^-) \\ &\quad + ip \frac{\Gamma}{3} \left[ \sum_{q,r} E_q^+ E_r^+ \bar{E}_{q+r-p}^+ + 2E_0^- \sum_q E_q^+ \bar{E}_{q-p}^+ \right. \\ &\quad \left. + \sum_q E_q^- E_{-q}^- \bar{E}_{-p}^+ + \bar{E}_0^- \sum_q E_q^+ E_{p-q}^+ + 2 \sum_q |E_q^-|^2 E_p^+ \right]. \end{aligned}$$

Removing terms resonant with  $e^{ipt}$ , we obtain

$$(2.7b) \quad \begin{aligned} -(\partial_T - \partial_Z)E_{-p}^- &= ip(N_{2p}E_{-p}^+ + N_0E_{-p}^-) \\ &+ ip\frac{\Gamma}{3} \left[ \sum_{q,r} E_q^- E_r^- \bar{E}_{q+r+p}^- + 2E_0^+ \sum_q E_q \bar{E}_{p+q}^- \right. \\ &\left. + \sum_q E_q^+ E_{-q}^+ \bar{E}_p^- + \bar{E}_0^+ \sum_q E_q \bar{E}_{-p-q}^+ + 2 \sum_q |E_q^+|^2 E_{-p}^- \right], \end{aligned}$$

where we have set  $\Gamma \equiv 3\chi/2$  to be consistent with previous work [14, 21]. Exchanging  $p$  for  $-p$  in (2.7b), we have

$$\begin{aligned} (\partial_T - \partial_Z)E_p^- &= ip(N_{-2p}E_p^+ + N_0E_p^-) \\ &+ ip\frac{\Gamma}{3} \left[ \sum_{q,r} E_q^- E_r^- \bar{E}_{q+r-p}^- + 2E_0^+ \sum_q E_q \bar{E}_{-p+q}^- \right. \\ &\left. + \sum_q E_q^+ E_{-q}^+ \bar{E}_{-p}^- + \bar{E}_0^+ \sum_q E_q \bar{E}_{p-q}^+ + 2 \sum_q |E_q^+|^2 E_p^- \right]. \end{aligned}$$

At  $p = 0$ , (2.7) can be satisfied by choosing arbitrary functions  $E_0^\pm = E_0^\pm(Z \mp T)$ . For simplicity, we set  $E_0^\pm(Z \mp T) \equiv 0$ . If we additionally use relations (2.6), then equations (2.7) simplify to xNLCME (1.10) from the introduction. Recall that we have set  $v_g = 1$ . Subject to constraints (2.7),  $E_p^{(1)}$ , the correction, can be obtained from a linear inhomogeneous equation as a bounded oscillatory function in  $t$ .

Note that the nonlocal system (1.8) can be recovered via the relations (1.9), with the inverse

$$(2.8) \quad E_p^\pm(Z, T) = \frac{1}{2\pi} \int_{-\pi}^{\pi} E^\pm(Z, T, \phi) e^{\mp ip\phi} d\phi.$$

The constraints (2.6) imply that  $E^\pm$  are real-valued. To construct the primitive electric field variables,  $E^\pm(Z, T, \phi_\pm)$  must be evaluated at different phases,  $\phi_\pm = z \mp t$ .

**2.2. Hamiltonian structure of xNLCME.** Let  $E_0^\pm = 0$ , and define  $H = \int_{\mathbb{R}} \mathcal{H} dZ$ , where the Hamiltonian density is given by

$$(2.9) \quad \begin{aligned} \mathcal{H} &= \frac{i}{2} \sum_p \frac{1}{p} (E_p^+ \partial_Z \bar{E}_p^+ - E_p^- \partial_Z \bar{E}_p^- - \bar{E}_p^+ \partial_Z E_p^+ + \bar{E}_p^- \partial_Z E_p^-) \\ &- N_0 \sum_p (|E_p^+|^2 + |E_p^-|^2) - \sum_p N_{2p} (\bar{E}_{-p}^- E_{-p}^+ + E_p^- \bar{E}_p^+) \\ &- \frac{\Gamma}{6} \left( \sum_p \bar{E}_p^+ \bar{E}_{-p}^+ \right) \left( \sum_p E_p^- E_{-p}^- \right) - \frac{\Gamma}{6} \left( \sum_p \bar{E}_p^- \bar{E}_{-p}^- \right) \left( \sum_p E_p^+ E_{-p}^+ \right) \\ &- \frac{\Gamma}{6} \sum_{p,q,r} (\bar{E}_p^+ E_q^+ E_r^+ \bar{E}_{q+r-p}^+ + \bar{E}_p^- E_q^- E_r^- \bar{E}_{q+r-p}^-) - \frac{2\Gamma}{3} \left( \sum_p |E_p^+|^2 \right) \left( \sum_p |E_p^-|^2 \right), \end{aligned}$$

where all sums are over  $\mathbb{Z} \setminus \{0\}$ . Then xNLCME has the structure of an infinite dimensional Hamiltonian system:

$$(2.10) \quad \partial_T E_p^+ = -ip \frac{\delta H}{\delta \bar{E}_p^+}, \quad \partial_T E_p^- = -ip \frac{\delta H}{\delta \bar{E}_p^-}, \quad p \in \mathbb{Z} \setminus \{0\}.$$

Formally, the Hamiltonian (2.9) is conserved under the flow of xNLCME. Besides the Hamiltonian, the total power  $N = \int_{\mathbb{R}} \mathcal{N} dZ$  is invariant, where the density is

$$(2.11) \quad \mathcal{N} = \sum_{p \in \mathbb{Z}} \left( |E_p^+|^2 + |E_p^-|^2 \right).$$

This follows by direct computation.

Since  $N_{2p} = \bar{N}_{-2p}$ ,  $p \in \mathbb{Z}$ , the symmetry of equations (1.10) implies that if the constraint (2.6), associated with real initial conditions for  $E^\pm$ , is satisfied at  $T = 0$ , then it is satisfied for all  $T$ . Additionally, if  $E_p^\pm$  are zero initially for even  $p$ , they remain zero for all time. This allows us to restrict (1.10) to the odd harmonics,  $p \in \mathbb{Z}_{\text{odd}}$ , and set

$$(2.12) \quad E_p^\pm = 0, \quad p \in \mathbb{Z}_{\text{even}}.$$

Constraints (2.12) arise naturally for initial data which contains only the first harmonic. Due to the cubic nonlinearity, this generates coupling of all odd (but not even) harmonics. In what follows, we simplify details of computations by assuming (2.12).

Under constraints (2.6), the conserved Hamiltonian density (2.9) reduces as follows:

$$(2.13) \quad \begin{aligned} \mathcal{H} = & \frac{i}{2} \sum_{p \in \mathbb{Z}} \frac{1}{p} \left( E_p^+ \partial_Z \bar{E}_p^+ - E_p^- \partial_Z \bar{E}_p^- - \bar{E}_p^+ \partial_Z E_p^+ + \bar{E}_p^- \partial_Z E_p^- \right) \\ & - N_0 \sum_{p \in \mathbb{Z}} \left( |E_p^+|^2 + |E_p^-|^2 \right) - 2 \sum_{p \in \mathbb{Z}} N_{2p} E_p^- \bar{E}_p^+ \\ & - \Gamma \left( \sum_{p \in \mathbb{Z}} |E_p^+|^2 \right) \left( \sum_{p \in \mathbb{Z}} |E_p^-|^2 \right) \\ & - \frac{\Gamma}{6} \sum_{p, q, r \in \mathbb{Z}} \left( \bar{E}_p^+ E_q^+ E_r^+ \bar{E}_{q+r-p}^+ + \bar{E}_p^- E_q^- E_r^- \bar{E}_{q+r-p}^- \right). \end{aligned}$$

As in the case of standard NLCME, (2.13) is unbounded from above and below subject to the constraint of fixed  $\mathcal{N}$ . Thus, critical points are expected to be of *infinite index*. This suggests that variational methods will be of limited applicability for studying the stability of localized stationary states of xNLCME.

**3. Gap solitons.** We now begin to explore the existence of localized stationary states of xNLCME (1.10) called *gap solitons*. Setting  $v_g = 1$  for convenience, we seek solutions of the form

$$(3.1) \quad E_p^+(Z, T) = e^{ip(N_0 - \Omega)T} A_p(Z), \quad E_p^-(Z, T) = e^{ip(N_0 - \Omega)T} B_p(Z), \quad p \in \mathbb{Z},$$



where  $\Omega$  is a real frequency parameter and  $\{A_p(Z), B_p(Z)\}_{p \in \mathbb{Z}}$  are complex-valued amplitudes. Using constraints (2.6) and (2.12), we assume

$$(3.2) \quad A_p = \bar{A}_{-p}, \quad B_p = \bar{B}_{-p}, \quad p \in \mathbb{Z}_{\text{odd}}, \quad A_p = B_p = 0, \quad p \in \mathbb{Z}_{\text{even}}.$$

The infinite family of amplitudes  $\{A_p, B_p\}_{p \in \mathbb{Z}_{\text{odd}}}$  satisfies the extended system of stationary equations

$$(3.3a) \quad iA'_p(Z) + p\Omega A_p + pN_{2p}B_p + p\frac{\Gamma}{3} \left( 3A_p \sum_{q \in \mathbb{Z}_{\text{odd}}} |B_q|^2 + \sum_{q,r \in \mathbb{Z}_{\text{odd}}} A_q A_r A_{p-q-r} \right) = 0,$$

$$(3.3b) \quad -iB'_p(Z) + p\Omega B_p + p\bar{N}_{2p}A_p + p\frac{\Gamma}{3} \left( 3B_p \sum_{q \in \mathbb{Z}_{\text{odd}}} |A_q|^2 + \sum_{q,r \in \mathbb{Z}_{\text{odd}}} B_q B_r B_{p-q-r} \right) = 0,$$

with constraints (3.2). Linearizing about the zero solution yields decoupled systems of differential equations with solutions

$$(3.4) \quad \begin{bmatrix} A_p \\ B_p \end{bmatrix} \sim e^{\pm pZ \sqrt{|N_{2p}|^2 - \Omega^2}}, \quad p \in \mathbb{Z}_{\text{odd}}.$$

A necessary condition for the existence of a solution which decays exponentially fast to zero as  $|Z| \rightarrow \infty$  is

$$(3.5) \quad |\Omega| < \Omega_0 \equiv \inf_{p \in \mathbb{Z}_{\text{odd}}} |N_{2p}|.$$

We consider three possibilities:

*Case 1:*  $\Omega_0 > 0$ . For example, let  $N_{2p} = 1, p \in \mathbb{Z}_{\text{odd}}$ . In this case,  $N(z)$  is a periodic sequence of Dirac delta-functions.

*Case 2:*  $\Omega_0 = 0$  and  $\inf_{p \in \mathbb{Z}_{\text{odd}}} |pN_{2p}| > 0$ . For example, let  $N_{2p} = p^{-1}, p \in \mathbb{Z}_{\text{odd}}$ . In this case,  $N(z)$  is the periodic extension of a step function.

*Case 3:*  $\Omega_0 = 0$  and  $\inf_{p \in \mathbb{Z}_{\text{odd}}} |p^2 N_{2p}| < \infty$ . In this case,  $N(z)$  is continuous.

If  $N_{2p} = 1, p \in \mathbb{Z}_{\text{odd}}$ , a spectral band gap for each mode is opened, and the widths of the band gaps grow as  $|p| \rightarrow \infty$ . However, because of the coupling between the Fourier modes with amplitudes  $\{A_p, B_p\}_{p \in \mathbb{Z}_{\text{odd}}}$ , the stationary localized mode (gap soliton) may reside only in the gap of a fixed width,  $\Omega \in (-\Omega_0, \Omega_0)$ , where  $\Omega_0 = \inf_{p \in \mathbb{Z}_{\text{odd}}} |N_{2p}| = 1$ .

If  $N_{2p} = \mathcal{O}(|p|^{-1})$ , the band gap of each mode is opened again, but the widths are nearly constant as  $|p| \rightarrow \infty$ . However, the band gap  $(-\Omega_0, \Omega_0)$  for the coupled gap soliton now shrinks to zero as  $\Omega_0 = \inf_{p \in \mathbb{Z}_{\text{odd}}} |N_{2p}| = 0$ , and the parameter  $\Omega$  must be set to 0.

If  $N_{2p} = \mathcal{O}(|p|^{-2})$ , the widths of the band gaps shrink with the larger values of  $p$ , and the exponential decay (3.4) ceases as  $|p| \rightarrow \infty$ , even if  $\Omega = 0$ . We do not anticipate the existence of gap solitons in this case.

We now restrict our attention to Case 1:  $\Omega_0 > 0$ , and we set  $N_{2p} = 1$  for all  $p \in \mathbb{Z}_{\text{odd}}$ . System (3.3) can now be rewritten as an equivalent integro-differential equation:

$$(3.6a) \quad (-\partial_Z + \Omega \partial_\phi)A + \partial_\phi B + \frac{\Gamma}{3} \partial_\phi \left[ A^3 + 3 \left( \frac{1}{2\pi} \int_{-\pi}^\pi |B(Z, s)|^2 ds \right) A \right] = 0,$$

$$(3.6b) \quad (\partial_Z + \Omega \partial_\phi)B + \partial_\phi A + \frac{\Gamma}{3} \partial_\phi \left[ B^3 + 3 \left( \frac{1}{2\pi} \int_{-\pi}^\pi |A(Z, s)|^2 ds \right) B \right] = 0,$$

where

$$(3.7) \quad A(Z, \phi) = \sum_{p \in \mathbb{Z}_{\text{odd}}} A_p(Z) e^{ip\phi}, \quad B(Z, \phi) = \sum_{p \in \mathbb{Z}_{\text{odd}}} B_p(Z) e^{ip\phi}.$$

As we commented earlier, if one wishes to compute the associated field induced by these envelopes, care must be taken in where the phase variable,  $\phi$ , is evaluated. Indeed, for the electric field associated with  $\{A_p, B_p\}_{p \in \mathbb{Z}_{\text{odd}}}$  we have

$$(3.8) \quad \begin{aligned} E(z, t) &= \epsilon^{\frac{1}{2}} \left[ \sum_{p \in \mathbb{Z}_{\text{odd}}} e^{ip(N_0 - \Omega)\epsilon t} e^{ip(z-t)} A_p(\epsilon z) + \sum_{p \in \mathbb{Z}_{\text{odd}}} e^{ip(N_0 - \Omega)\epsilon t} e^{-ip(z+t)} B_p(\epsilon z) + \mathcal{O}(\epsilon) \right] \\ &= \epsilon^{\frac{1}{2}} [A(\epsilon z, (N_0 - \Omega)\epsilon t + z - t) + B(\epsilon z, (N_0 - \Omega)\epsilon t - (z + t)) + \mathcal{O}(\epsilon)], \end{aligned}$$

in agreement with the ansatz (1.7).

**3.1. NLCME gap solitons.** As noted, the truncation of xNLCME to only one mode,  $E_1^\pm$ , yields the classical NLCME. We now review the details of the NLCME gap soliton.

The spatial profiles of NLCME's gap soliton are given by solutions of the stationary equations

$$(3.9a) \quad iA_1'(Z) + \Omega A_1 + B_1 + \Gamma(|A_1|^2 + 2|B_1|^2)A_1 = 0,$$

$$(3.9b) \quad -iB_1'(Z) + \Omega B_1 + A_1 + \Gamma(2|A_1|^2 + |B_1|^2)B_1 = 0.$$

For  $\Omega \in (-1, 1)$ , these equations admit the exact solutions

$$(3.10a) \quad A_1(Z) = \sqrt{\frac{2}{3\Gamma}} \frac{\mu}{\alpha \cosh(\mu Z) - i\beta \sinh(\mu Z)},$$

$$(3.10b) \quad B_1(Z) = \sqrt{\frac{2}{3\Gamma}} \frac{-\mu}{\alpha \cosh(\mu Z) + i\beta \sinh(\mu Z)},$$

where

$$\alpha = \sqrt{1 + \Omega}, \quad \beta = \sqrt{1 - \Omega}, \quad \mu = \sqrt{1 - \Omega^2} \equiv \alpha\beta.$$

The localized solution (3.10) satisfies the symmetry property

$$A_1(Z) = \bar{A}_1(-Z), \quad B_1(Z) = \bar{B}_1(-Z), \quad Z \in \mathbb{R}.$$

We shall call the solution of (3.10) a *monochromatic gap soliton*, since the associated approximate solution of the nonlinear Maxwell model consists of a slowly varying and localized envelope with a single fast (carrier) frequency of oscillation. This is in contrast to the broad band, or polychromatic, solitons which possess slowly varying envelopes on multiple distinct carrier frequencies. It seems unlikely that there is an explicit solution of the system (3.3) of infinitely many coupled mode equations.

**3.2. Persistence of solitons in a band edge approximation.** We now explore a small amplitude, spectral band edge approximation of xNLCME, which will lead to an infinite system of coupled NLS-type equations, xNLS.

**3.2.1. The band edge approximation.** The gap in the continuous spectrum exists for  $\Omega \in (-1, 1)$ . In the truncated coupled mode equations (3.9), the exact solution (3.10) shows that the amplitude  $\|A_1\|_{L^\infty}$  of the gap soliton tends to zero as  $\Omega \rightarrow 1$ . Using the parameterization  $\Omega = \sqrt{1 - \mu^2}$  with  $\mu$  small and the asymptotic expansion

$$(3.11a) \quad A_1 = \mu U_1(\mu Z) + \mathcal{O}(\mu^2) = \mu U_1(\zeta) + \mathcal{O}(\mu^2),$$

$$(3.11b) \quad B_1 = -\mu U_1(\mu Z) + \mathcal{O}(\mu^2) = -\mu U_1(\zeta) + \mathcal{O}(\mu^2),$$

we find

$$(3.12) \quad U_1''(\zeta) - U_1(\zeta) + 6\Gamma U_1^3(\zeta) = 0.$$

This equation admits the localized solution

$$(3.13) \quad U_*(\zeta) = \frac{1}{\sqrt{3\Gamma}} \operatorname{sech}(\zeta),$$

which, together with (3.11), gives an asymptotic approximation of the gap soliton (3.10) as  $\Omega \rightarrow 1$ . We now generalize this approach to the system of infinitely many coupled mode equations (3.3). Let

$$(3.14) \quad \Omega = \sqrt{1 - \mu^2}, \quad A_p = \mu \tilde{A}_p(\zeta), \quad B_p = -\mu \tilde{B}_p(\zeta), \quad p \in \mathbb{Z}_{\text{odd}}, \quad \zeta = \mu Z.$$

Substitution of (3.14) into the coupled mode system (3.3) yields

$$(3.15a) \quad i\mu \tilde{A}'_p + p\sqrt{1 - \mu^2} \tilde{A}_p - p\tilde{B}_p + \frac{p}{3}\Gamma \mu^2 \tilde{F}_p = 0,$$

$$(3.15b) \quad i\mu \tilde{B}'_p - p\sqrt{1 - \mu^2} \tilde{B}_p + p\tilde{A}_p - \frac{p}{3}\Gamma \mu^2 \tilde{G}_p = 0,$$

where

$$(3.16a) \quad \tilde{F}_p = 3\tilde{A}_p \sum_{q \in \mathbb{Z}_{\text{odd}}} |\tilde{B}_q|^2 + \sum_{q,r \in \mathbb{Z}_{\text{odd}}} \tilde{A}_q \tilde{A}_r \tilde{A}_{p-q-r},$$

$$(3.16b) \quad \tilde{G}_p = 3\tilde{B}_p \sum_{q \in \mathbb{Z}_{\text{odd}}} |\tilde{A}_q|^2 + \sum_{q,r \in \mathbb{Z}_{\text{odd}}} \tilde{B}_q \tilde{B}_r \tilde{B}_{p-q-r}.$$

Introducing the variables

$$\tilde{U}_p = \frac{\tilde{A}_p + \tilde{B}_p}{2}, \quad \tilde{V}_p = \frac{\tilde{A}_p - \tilde{B}_p}{2},$$

the system (3.15) can be written as

$$(3.17a) \quad 2p\tilde{V}_p + i\mu\tilde{U}'_p + \left(\sqrt{1 - \mu^2} - 1\right)p\tilde{V}_p + \frac{1}{6}\Gamma\mu^2 p(\tilde{F}_p - \tilde{G}_p) = 0,$$

$$(3.17b) \quad i\tilde{V}'_p + \frac{\sqrt{1 - \mu^2} - 1}{\mu} p\tilde{U}_p + \frac{1}{6}\Gamma\mu p(\tilde{F}_p + \tilde{G}_p) = 0,$$

where  $\tilde{F}_p, \tilde{G}_p$  can be expressed in terms of  $\tilde{U}_p$  and  $\tilde{V}_p$ .

Formally expanding in powers of  $\mu$ ,

$$(3.18) \quad \tilde{U}_p = U_p + \mathcal{O}(\mu^1), \quad \tilde{V}_p = -\frac{i\mu}{2p}U'_p + \mathcal{O}(\mu^2),$$

we obtain, at leading order, an infinite system of coupled NLS-type equations that we deem xNLS:

$$(3.19) \quad U''_p(\zeta) - p^2U_p + \frac{2p^2}{3}\Gamma \left( 3U_p \sum_{q \in \mathbb{Z}_{\text{odd}}} |U_q|^2 + \sum_{q \in \mathbb{Z}_{\text{odd}}} \sum_{r \in \mathbb{Z}_{\text{odd}}} U_q U_r U_{p-q-r} \right) = 0, \quad p \in \mathbb{Z}_{\text{odd}}.$$

This can be rewritten as the integro-differential equation

$$(3.20) \quad (\partial_\zeta^2 + \partial_\phi^2)U = \frac{2}{3}\Gamma \partial_\phi^2 \left[ U^3 + 3 \left( \frac{1}{2\pi} \int_{-\pi}^\pi |U(\zeta, \theta)|^2 d\theta \right) U \right]$$

after introducing the Fourier relations

$$U(\zeta, \phi) = \sum_{p \in \mathbb{Z}_{\text{odd}}} U_p(\zeta)e^{ip\phi}, \quad U_p(\zeta) = \frac{1}{2\pi} \int_{-\pi}^\pi U(\zeta, \phi)e^{-ip\phi} d\phi.$$

We will now justify the reduction to xNLS (3.19).

**3.2.2. Preliminaries.** We first introduce appropriate function spaces. Let  $\mathbb{T}$  denote the interval  $[0, 2\pi]$ , with endpoints identified so that functions on  $\mathbb{T}$  are understood to be  $2\pi$ -periodic. We shall consider functions defined on  $\mathbb{R} \times \mathbb{T}$ , admitting the Fourier representation

$$U(\zeta, \phi) = \sum_{p \in \mathbb{Z}_{\text{odd}}} U_p(\zeta)e^{ip\phi}.$$

For any  $s$ , the function space  $X^s$  is defined by

$$(3.21) \quad X^s \equiv \left\{ U(\zeta, \phi) \in H^s(\mathbb{R} \times \mathbb{T}) : \begin{array}{l} \bar{U}(\zeta, \phi) = U(\zeta, \phi), \\ \int_{-\pi}^\pi U(\zeta, \phi) \cos(2p\phi) d\phi = 0 \quad \forall \zeta \in \mathbb{R}, p \in \mathbb{Z}_{\text{odd}} \end{array} \right\},$$

equipped with the norm

$$(3.22) \quad \|U\|_{X^s} \equiv \left( \sum_{p \in \mathbb{Z}_{\text{odd}}} \int_{\mathbb{R}} (p^2 + \xi^2)^s |\widehat{U}_p(\xi)|^2 d\xi \right)^{1/2},$$

where  $\widehat{U}_p(\xi)$  is the Fourier transform of  $U_p(\zeta)$  in the  $\zeta$ . We shall frequently go back and forth between the  $U$  and  $\{U_p\}_{p \in \mathbb{Z}_{\text{odd}}}$  representations of functions in  $X^s$ .

The Sobolev space  $H^s(\mathbb{R} \times \mathbb{T})$  is a Banach algebra with respect to pointwise multiplication for any  $s > 1$ . Moreover, we recall the continuous embeddings  $H^s(\mathbb{R} \times \mathbb{T}) \hookrightarrow C(\mathbb{R} \times \mathbb{T})$  for  $s > 1$  and  $l^2(\mathbb{Z}) \hookrightarrow l^\infty(\mathbb{Z})$ . In particular if  $U \in X^s$  for  $s > 1$ , then

$$(3.23) \quad \lim_{|\zeta| \rightarrow \infty} U(\zeta, \phi) = 0 \quad \forall \phi \in \mathbb{T}.$$

Let  $B_\delta(X^s)$  denote a ball of radius  $\delta$  in Banach space  $X^s$  centered at the origin. The Hamiltonian  $H$  with the density (2.13) consists of the terms controlled by the  $H^1$  norms of  $E^\pm$ . To see this, recall the continuous embedding  $H^1(\mathbb{R} \times \mathbb{T}) \hookrightarrow L^4(\mathbb{R} \times \mathbb{T})$ . It follows that for any  $E^\pm \in B_\delta(X^s)$  with  $s \geq 1$ , there is a constant  $C_{\delta,s} > 0$  such that

$$H \leq C_{\delta,s} (\|E^+\|_{X^s} + \|E^-\|_{X^s}).$$

Furthermore, the map  $(E^+, E^-) \mapsto H$  is continuously differentiable in  $X^s$ . Although we will mainly study the problem in  $X^s$  with  $s > 1$ , we note that the energy is well defined in  $X^1$ .

**3.2.3. Proof of result.** We now justify the small amplitude approximation of (3.3) by (3.19). We assume existence of a localized solution  $U \in X^s$ ,  $s > 1$ , in the integro-differential equation (3.20). The existence of  $U \in X^s$  is an open problem. However, numerical evidence of the existence of solutions can be found in section 5.1.

We also assume invertibility of a linearized operator associated with system (3.20). This assumption is standard in the persistence analysis, and it is often checked numerically; see [9, 10] for similar studies.

**Theorem 3.1.** *Fix  $s > 1$  and assume the existence of localized solution  $U \in X^s$  to (3.20) satisfying the reversibility symmetry,*

$$(3.24) \quad U_p(\zeta) = \bar{U}_p(-\zeta), \quad p \in \mathbb{Z}_{\text{odd}}, \quad \zeta \in \mathbb{R}.$$

Also assume that the linearized operator of system (3.20) at  $U$  is invertible in the subspace of  $X^s$  associated with the constraint (3.24).

There exists  $\mu_0 > 0$  such that for any  $\mu \in (-\mu_0, \mu_0)$ , the system of stationary coupled mode equations (3.3) with  $\Omega = \sqrt{1 - \mu^2}$  admits a unique localized solution  $A, B \in X^s$  satisfying the symmetries,

$$(3.25) \quad A_p(Z) = \bar{A}_p(-Z), \quad B_p(z) = \bar{B}_p(-Z), \quad p \in \mathbb{Z}_{\text{odd}}, \quad Z \in \mathbb{R},$$

and the bound,

$$(3.26) \quad \|A - \mu U(\mu \cdot, \cdot)\|_{X^s} + \|B + \mu U(\mu \cdot, \cdot)\|_{X^s} \leq C\mu^2.$$

*Proof.* First, we note that the vector fields  $\tilde{F}(A, B)$  and  $\tilde{G}(A, B)$ , defined by their components in (3.16), are analytic (cubic) maps from  $X^s \times X^s$  to  $X^s$  for any  $s > 1$ . Eliminating  $\tilde{U}_p$  from system (3.17), we obtain

$$(3.27) \quad p^2 \tilde{V}_p - \tilde{V}_p'' = \frac{1}{6} \Gamma \left[ p^2 (\sqrt{1 - \mu^2} - 1) (\tilde{F}_p - \tilde{G}_p) - i\mu p (\tilde{F}_p' + \tilde{G}_p') \right].$$

The right-hand side of system (3.27) defines an analytic (cubic) map from  $X^s$  to  $X^{s-2}$  for any  $s > 1$ , where the  $X^{s-2}$  norm is of order  $\mathcal{O}(\mu)$  as  $\mu \rightarrow \infty$ . The left-hand side operator of system (3.27) has a bounded inverse from  $X^{s-2}$  to  $X^s$ , thanks to the zero mean constraint in  $X^s$ . By the implicit function theorem, we infer that for any  $\delta > 0$  and any  $s > 1$ , there is  $\mu_0 > 0$  such that for all  $\mu \in (-\mu_0, \mu_0)$  and for all  $\tilde{U}$  in a ball  $B_\delta(X^s)$ , there is a smooth map  $X^s \ni \tilde{U} \mapsto \tilde{V}[\tilde{U}] \in X^s$  which solves system (3.27) and satisfies the bound,

$$(3.28) \quad \exists C > 0: \quad \|\tilde{V}\|_{X^s} \leq C\mu, \quad \mu \in (-\mu_0, \mu_0), \quad \tilde{U} \in B_\delta(X^s).$$

On the other hand, eliminating  $\tilde{V}$  from system (3.17), we obtain

$$(3.29) \quad \tilde{U}_p'' - p^2 \tilde{U}_p + \frac{1}{6} \Gamma \left[ p^2 (\sqrt{1 - \mu^2} + 1) (\tilde{F}_p + \tilde{G}_p) - i \mu p (\tilde{F}_p' - \tilde{G}_p') \right] = 0.$$

By the bound (3.28), the cubic terms of the system (3.29) are equal to those of (3.19) plus an error of the order of  $\mathcal{O}(\mu^2)$  in  $X^{s-2}$ . Under the assumptions of the existence of the solution  $U \in X^s$  of the truncated coupled NLS equations (3.20) and the invertibility of the linearized operator in the subspace of  $X^s$  associated with the constraint (3.24), the linearized operator has a bounded inverse from  $X^{s-2}$  to  $X^s$  for any small  $\mu \in \mathbb{R}$ . By the contraction mapping arguments, there is a solution  $\tilde{U}$  near  $U$  in  $X^s$  such that

$$\exists C > 0: \quad \|\tilde{U} - U\|_{X^s} \leq C \mu^2.$$

This gives the statement of the theorem, after the original variables  $A$ ,  $B$ , and  $Z$  are restored from the transformations above. ■

**3.3. Hamiltonian and power of xNLS.** The extended system of coupled nonlinear Schrödinger equations (xNLS) (3.19) inherits the Hamiltonian structure of the coupled mode equations (3.3). The energy functional for (3.19) is given by

$$(3.30) \quad H_{\text{xNLS}} = \int_{\mathbb{R}} \left[ \sum_{p \in \mathbb{Z}_{\text{odd}}} \left( \frac{1}{p^2} |U_p'|^2 + |U_p|^2 \right) - \Gamma \left( \sum_{p \in \mathbb{Z}_{\text{odd}}} |U_p|^2 \right)^2 - \frac{\Gamma}{3} \sum_{p, q, r \in \mathbb{Z}_{\text{odd}}} \bar{U}_p U_q U_r \bar{U}_{q+r-p} \right] d\zeta.$$

We also define the power,

$$(3.31) \quad N_{\text{xNLS}} = \int_{\mathbb{R}} \left[ \sum_{p \in \mathbb{Z}} |U_p|^2 \right] d\zeta.$$

Energy functionals are often used in proving the existence of localized solutions to constrained variational problems, e.g.,

$$(3.32) \quad \text{minimize } H_{\text{xNLS}} \text{ subject to fixed } N_{\text{xNLS}}.$$

Unfortunately, this strategy fails for our problem, as demonstrated by the following counterexample. Let

$$(3.33) \quad U_p(\zeta) = \lambda_n^{1/2} W(\lambda_n \zeta) (\delta_{p,n} + \delta_{p,-n}), \quad p \in \mathbb{Z}_{\text{odd}},$$

where  $W \in H^1(\mathbb{R})$  is a fixed function,  $\lambda_n > 0$  is an arbitrary parameter, and  $n \geq 1$  is an arbitrary odd integer. Then,  $N_{\text{xNLS}}$  is independent of the parameters  $\lambda_n$  and  $n$ . On the other hand,

$$H_{\text{xNLS}} = \frac{2\lambda_n^2}{n^2} \|W'\|_{L^2}^2 - 6\lambda_n \|B\|_{L^4}^4.$$

If we set  $\lambda_n = n$  and let  $n \rightarrow \infty$ , we obtain no lower bound on  $H_{\text{xNLS}}$ . Thus, localized solutions of xNLS (3.19), if they exist in some  $X^s$ , cannot be global minimizers of  $H_{\text{xNLS}}$  subject to fixed  $N_{\text{xNLS}}$ ; they will be either local extrema or saddle points.

**3.4. Persistence of monochromatic solitons to coupling in xNLS.** We study the question of persistence of NLS solitons within xNLS by embedding xNLS in a one-parameter family of models,  $xNLS^\epsilon$ , for which  $xNLS^0$  is an infinite system of decoupled NLS equations and  $xNLS^1=xNLS$ :

$$(3.34) \quad U_p'' - p^2 U_p + 6p^2 \Gamma U_p^3 + \frac{2p^2}{3} \epsilon \Gamma \left( 3U_p \sum'_{q \in \mathbb{Z}_{\text{odd}}} |U_q|^2 + \sum'_{q,r \in \mathbb{Z}_{\text{odd}}} U_q U_r U_{p-q-r} \right) = 0, \quad p \in \mathbb{Z}_{\text{odd}},$$

where the  $\sum'$  indicates that the cubic self-interaction terms,  $U_p^3$ , are excluded. Within each mode of the decoupled system at  $\epsilon = 0$ , we have a solution

$$(3.35) \quad U_p(\zeta) = \pm U_\star(p\zeta), \quad p \in \mathbb{Z}_{\text{odd}},$$

where  $U_\star(\zeta)$  is the NLS soliton (3.13).

We now prove the persistence of the solution  $U_1^{\epsilon=0}(\zeta) = U_\star(\zeta)$  and  $U_p^{\epsilon=0} = 0$  for  $p \neq 1$  within  $xNLS^\epsilon$  (3.34) for all  $\epsilon$  sufficiently small. Furthermore, we make the reduction

$$U_p(\zeta) = \bar{U}_p(\zeta) = U_{-p}(\zeta), \quad p \in \mathbb{Z}_{\text{odd}}.$$

In other words, we now assume that the envelopes in each harmonic are real-valued.

**Theorem 3.2.** *Fix  $s > 1$ . There exist  $\epsilon_0 > 0$  and  $C > 0$  such that for any  $\epsilon \in (-\epsilon_0, \epsilon_0)$ , xNLS (3.34) admits a unique localized solution  $U \in X^s$  satisfying the even symmetry:*

$$(3.36) \quad U_p(\zeta) = U_p(-\zeta).$$

Moreover,  $U(\zeta, \phi)$  is a small deformation of the unperturbed  $\epsilon = 0$  soliton solution,

$$\mathcal{U}_\star(\zeta, \phi) = 2U_\star(\zeta) \cos(\phi),$$

in the sense that

$$(3.37) \quad \|U - \mathcal{U}_\star\|_{X^s} \leq C\epsilon.$$

*Proof.* The proof relies on a Lyapunov–Schmidt reduction, where we shall first express the higher harmonics as functions of  $U_1 = U_{-1}$  and then apply the implicit function theorem to an equation written entirely in terms of  $U_1$ .

From (3.34), define  $F$  in terms of the components

$$F_p = 3U_p \sum'_{q \in \mathbb{Z}_{\text{odd}}} |U_q|^2 + \sum'_{q,r \in \mathbb{Z}_{\text{odd}}} U_q U_r U_{p-q-r},$$

where each  $F_p$  excludes the purely self-interacting terms. We then have

$$(3.38) \quad U_p = -(\partial_\zeta^2 - p^2)^{-1} p^2 (6\Gamma U_p^3) - \epsilon (\partial_\zeta^2 - p^2)^{-1} p^2 \frac{2}{3} \Gamma F_p, \quad |p| > 1.$$

The terms on the right are in  $X^s$  since  $s > 1$  and  $(\partial_\zeta^2 - p^2)^{-1} p^2$  is a bounded operator. Therefore, for sufficiently small  $\epsilon_0 > 0$  and finite  $\delta_0$ , the contraction mapping theorem yields a unique map,

$$\Phi : (U_1, \epsilon) \mapsto \{U_p\}_{|p|>1},$$

in a ball  $U_1 \in B_\delta(H^s)$  with  $\delta < \delta_0$  and  $|\epsilon| < \epsilon_0$ . From (3.38), there exist constants  $C > 0$  and  $\epsilon_0 > 0$  such that for all  $|\epsilon| < \epsilon_0$ , (3.38) has a solution  $U_p = U_p[U_{\pm 1}]$ , for  $|p| > 1$ , satisfying the bound

$$\left\| \{U_p\}_{|p|>1} \right\|_{X^s} = \|\Phi(U_1, \epsilon)\|_{X^s} \leq C\epsilon \|U_1\|_{H^s}^3.$$

We now eliminate  $\{U_p\}_{|p|>1}$  from the  $p = \pm 1$  equations of (3.34) using the mapping  $\Phi$ . Since  $U_1 = U_{-1}$ , we consider only the  $p = 1$  equation:

$$(3.39) \quad \mathcal{M}[U_1, \epsilon] \equiv U_1'' - U_1 + 6\Gamma U_1^3 + \frac{2}{3}\epsilon\Gamma F_1[\Phi(U_1, \epsilon)] = 0.$$

For any  $U_1 \in B_\delta(H^s)$  with finite  $\delta > 0$  and small  $|\epsilon| < \epsilon_0$ , there is a  $C > 0$  such that

$$\|F_1[\Phi(U_1, \epsilon)]\|_{H^s} \leq C\epsilon \|U_1\|_{H^s}^5.$$

To solve (3.39), we apply the implicit function theorem. The key ingredient is to check that the linearization of  $\mathcal{M}$  at  $U_1 = U_\star$  and  $\epsilon = 0$ ,

$$d\mathcal{M}[U_\star, 0] = \partial_\zeta^2 - 1 + 18\Gamma U_\star^2,$$

is an invertible mapping from  $H_{\text{even}}^{s-2}$  to  $H_{\text{even}}^s$ , the subspace of  $H^s$  satisfying (3.36). It is simple to check that the null space of this operator is  $\text{span}\{\partial_\zeta U_\star\}$ . Since  $\partial_\zeta U_\star$  does not satisfy (3.36), the  $H_{\text{even}}^s$ -kernel of  $d\mathcal{M}[U_\star, 0] = \{0\}$  and  $d\mathcal{M}[U_\star, 0]$  is invertible. Hence, the implicit function theorem yields a neighborhood of  $U_\star$  in  $H^s$  in which we can obtain  $U_1$  with  $|\epsilon| < \epsilon_1 \leq \epsilon_0$ .

Moreover, we see from (3.39) that there exists  $C > 0$  such that for all  $|\epsilon| < \epsilon_1$ ,

$$\|U_1 - U_\star\|_{H^s} \leq C\epsilon^2.$$

Combining this estimate with the one derived from (3.38) yields (3.37). This completes the proof of Theorem 3.2.  $\blacksquare$

This result has several obvious extensions. We can consider the local continuation about a soliton localized in any other mode  $p_0 \in \mathbb{Z}_{\text{odd}}$ ,

$$(3.40) \quad U_{p_0}(\zeta) = \pm U_\star(p\zeta).$$

We could also continue a solution about any finite collection of such solitons, indexed by a set  $J$ . However, if we begin with solitons in any infinite subset of odd harmonics, they will not have finite  $L^2$  norm; i.e.,

$$\int \sum_{p \in J} |U_p|^2 d\zeta = \|U_\star\|_{L^2}^2 \sum_{p \in J} \frac{1}{|p|} = \infty.$$

The continuation of such infinite energy solutions is not covered by our analysis.

**4. Approximation of solutions via trial functions.** As noted at the end of section 3.2.3, although the functional is bounded from below, the natural variational formulation for localized solutions of xNLS exhibits a loss of compactness. In this section we use this functional to obtain approximations of critical points using parameterized trial functions.



**4.1. Gaussian approximations.** Let us consider the Gaussian variational ansatz

$$(4.1) \quad U_p(\zeta) = a_p e^{-b_p \zeta^2}, \quad p \in \mathbb{Z}_{\text{odd}},$$

where  $a_p \in \mathbb{R}$  and  $b_p \in \mathbb{R}_+$  are parameters to be determined. The Gaussian ansatz is useful because all integrals in  $H_{\text{xNLS}}$  can be computed in the analytical form. Although a sech-like ansatz may seem natural for approximating solitary waves with exponentially decaying tails, the integrals in  $H_{\text{xNLS}}$  for the nonlinear terms do not simplify for sech functions.

Direct substitution and integration show that  $\sqrt{\frac{2}{\pi}} H_{\text{xNLS}}$  becomes

$$(4.2) \quad H_{\text{Gauss}} = \sum_{p \in \mathbb{Z}_{\text{odd}}} \frac{\sqrt{b_p} a_p^2}{p^2} + \frac{a_p^2}{\sqrt{b_p}} - \Gamma \sum_{p,q \in \mathbb{Z}_{\text{odd}}} \frac{a_p^2 a_q^2}{\sqrt{b_p + b_q}} - \frac{1}{3} \Gamma \sum_{p,q,r \in \mathbb{Z}_{\text{odd}}} \frac{\sqrt{2} a_p a_q a_r a_{p-q-r}}{\sqrt{b_p + b_q + b_r + b_{p-q-r}}}.$$

Again, we introduce a parameter  $\epsilon$  in order to decouple the different modes, as in system (3.34). Equation (4.2) is then rewritten in the form

$$(4.3) \quad H_{\text{Gauss}}(\epsilon) \equiv \sum_{p \in \mathbb{Z}_{\text{odd}}} \frac{\sqrt{b_p} a_p^2}{p^2} + \frac{a_p^2}{\sqrt{b_p}} - \Gamma \frac{3a_p^4}{\sqrt{2}\sqrt{b_p}} - \epsilon \Gamma \left( \sum'_{p,q \in \mathbb{Z}_{\text{odd}}} \frac{a_p^2 a_q^2}{\sqrt{b_p + b_q}} + \frac{1}{3} \sum'_{p,q,r \in \mathbb{Z}_{\text{odd}}} \frac{\sqrt{2} a_p a_q a_r a_{p-q-r}}{\sqrt{b_p + b_q + b_r + b_{p-q-r}}} \right).$$

The sums  $\sum'$  exclude the purely self-interacting  $a_p^4/\sqrt{b_p}$  terms, and  $H_{\text{Gauss}}(1) = H_{\text{Gauss}}$ .

If  $\epsilon = 0$ , there exists an uncoupled solution of the Euler–Lagrange equations produced from variations of  $H_{\text{Gauss}}(0)$ ,

$$(4.4) \quad a_p = \pm \frac{2^{3/4}}{3\Gamma^{1/2}}, \quad b_p = \frac{p^2}{3}, \quad p \in \mathbb{Z}_{\text{odd}}.$$

The exact solution (4.4) will be used as a seed point in the numerical continuation algorithm.

**4.2. Numerical continuation.** Truncating  $H_{\text{Gauss}}(\epsilon)$  in (4.3) to resolve only  $N$  harmonics, we define  $H_{\text{Gauss}}^N(\mathbf{a}, \mathbf{b}, \epsilon)$ . The associated system of  $2N$  Euler–Lagrange equations is

$$(4.5) \quad \nabla_{\mathbf{a}} H_{\text{Gauss}}^N(\mathbf{a}, \mathbf{b}, \epsilon) = 0, \quad \nabla_{\mathbf{b}} H_{\text{Gauss}}^N(\mathbf{a}, \mathbf{b}, \epsilon) = 0.$$

We now seek solutions of the  $\epsilon = 0$  system, where all modes are decoupled, that can be continued to  $\epsilon = 1$ , the desired system. The natural family of solutions is given by (4.4). Thus, for our  $\epsilon = 0$  starting point, we consider solutions of the form

$$(4.6) \quad \mathbf{a}_* = \frac{2^{3/4}}{3\Gamma^{1/2}} (\sigma_1, \sigma_2, \dots, \sigma_N),$$

$$(4.7) \quad \mathbf{b}_* = \frac{1}{3} (1^2, 3^2, \dots, (2N - 1)^2),$$

where  $\sigma_j \in \{-1, 0, 1\}$ . The variances,  $\mathbf{b}_*$ , are unaffected by  $\boldsymbol{\sigma}$ . Indeed, for  $\sigma_j = 0$ ,  $b_j$  is ill-defined and can take any value.

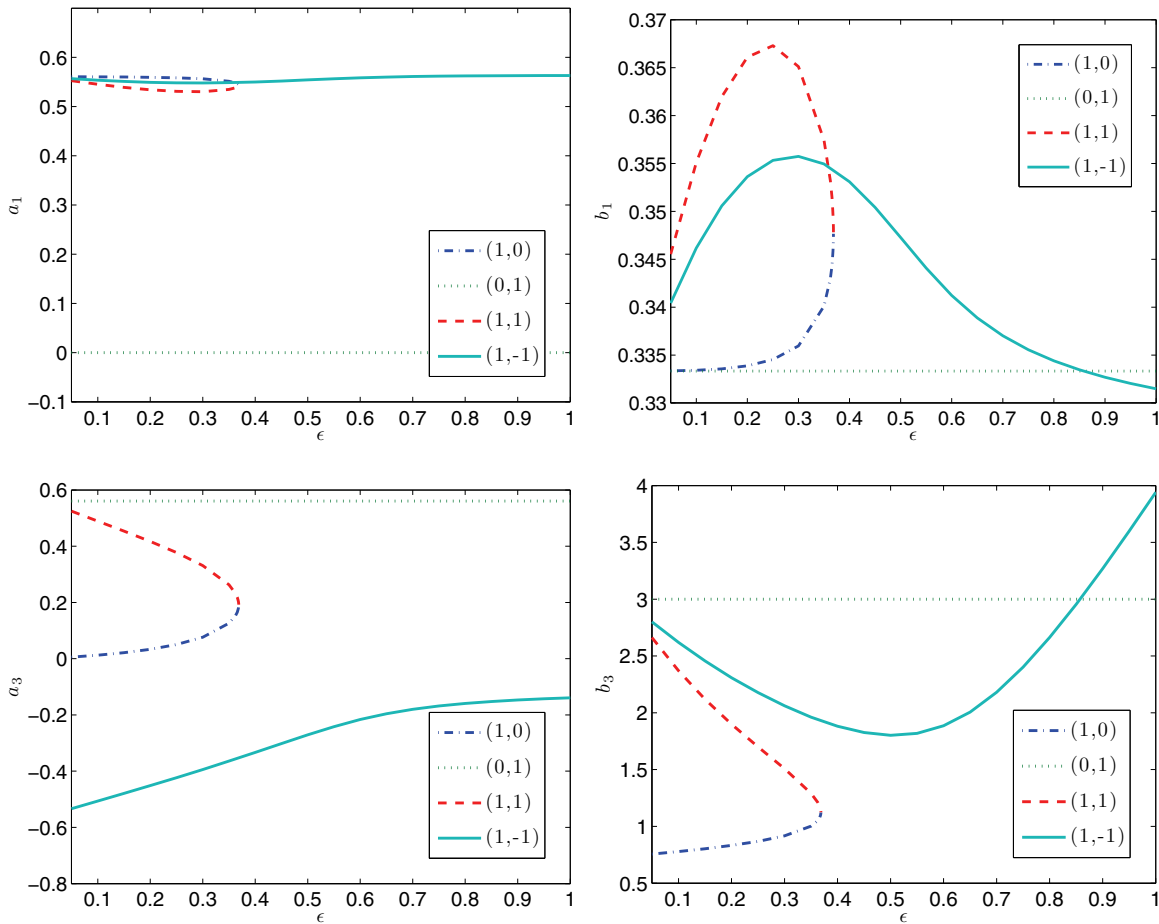


Figure 1. Various continuation branches for a two-mode trial function system.

We now explore continuations from various choices of  $\sigma$ 's. Before giving the results, we state the conjecture that our computations suggest.

**Conjecture 4.1.** For any  $N \geq 1$ , there is a nontrivial configuration  $\sigma$  that can be continued from  $\epsilon = 0$  to  $\epsilon = 1$ . At  $\epsilon = 1$ , the amplitudes are sign alternating:

$$\text{sign}(a_p) = (-1)^{(|p|-1)/2}.$$

For a system of two modes ( $N = 2$ ), the numerical continuation of four  $\sigma$  configurations is plotted in Figure 1. The configurations  $\sigma = (0, 1)$  and  $\sigma = (1, -1)$  can be continued to  $\epsilon = 1$ , while the other two collide and terminate near  $\epsilon = 0.368$ . Extending this to a system of three modes, we plot the analogous results in Figure 2. Three configurations  $\sigma = (0, 1, 0)$ ,  $\sigma = (0, 0, 1)$ , and  $\sigma = (1, -1, 1)$  can be continued to  $\epsilon = 1$ . We note that the configurations  $\sigma = (0, 1)$ ,  $\sigma = (0, 1, 0)$ , and  $\sigma = (0, 0, 1)$  are trivial in the sense that they are generated by the reductions of the truncated coupled NLS equations. When more modes are included in the system, these degenerate configurations are destroyed. On the other hand, the configurations  $\sigma = (1, -1), (1, -1, 1)$  are nontrivial and persist with respect to adding more modes in the

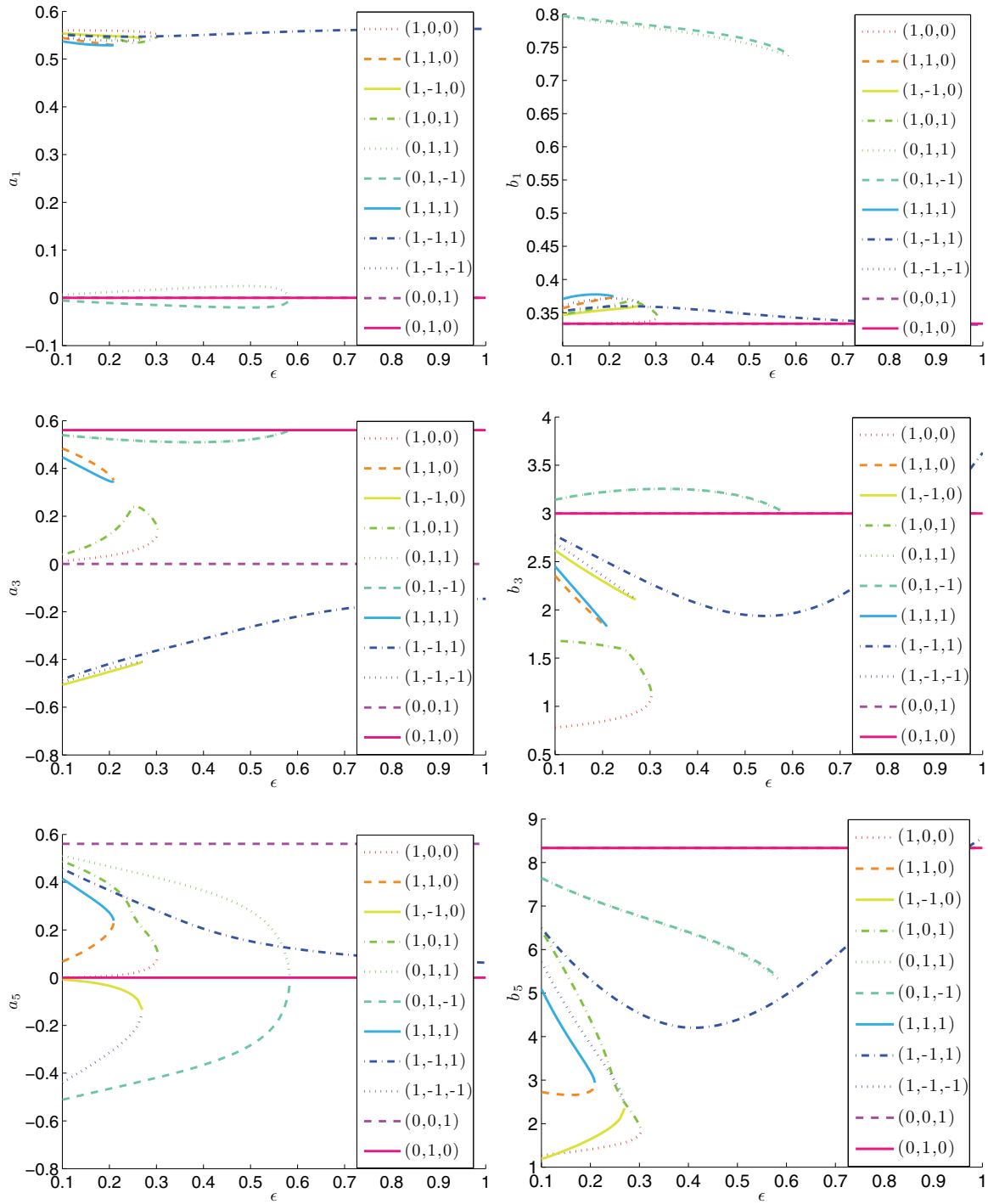


Figure 2. Various continuation branches for a three-mode trial function system.

**Table 1**

Computed values for a truncated trial function approximation for  $\epsilon = 1$ .

| No. of modes | $a_1$   | $b_1$   | $a_3$    | $b_3$  | $a_5$    | $b_5$  |
|--------------|---------|---------|----------|--------|----------|--------|
| 1            | 0.56060 | 0.33333 | -        | -      | -        | -      |
| 2            | 0.56321 | 0.33148 | -0.13918 | 3.9413 | -        | -      |
| 3            | 0.56329 | 0.33189 | -0.14585 | 3.6287 | 0.062822 | 8.5577 |

**Table 2**

Computed values for a truncated trial function approximation with fixed  $\mathbf{b}_*$  for  $\epsilon = 1$ . The branch from which we continue is alternating for  $1 \leq N \leq 4$ :  $\boldsymbol{\sigma} = (1), (1, -1), (1, -1, 1), (1, -1, 1, -1)$ . The case  $N = 5$  is continued from the branch  $(1, -1, 1, 1, 1)$ , and  $N = 6$  is continued from  $(1, -1, 1, -1, -1, -1)$ .

| No. of modes | $a_1$   | $a_3$    | $a_5$    | $a_7$     | $a_9$    | $a_{11}$  |
|--------------|---------|----------|----------|-----------|----------|-----------|
| 1            | 0.56060 | -        | -        | -         | -        | -         |
| 2            | 0.5643  | -0.12734 | -        | -         | -        | -         |
| 3            | 0.56409 | -0.13759 | 0.061454 | -         | -        | -         |
| 4            | 0.56386 | -0.14037 | 0.068618 | -0.037695 | -        | -         |
| 5            | 0.56372 | -0.14139 | 0.071254 | -0.042822 | 0.026041 | -         |
| 6            | 0.56364 | -0.14184 | 0.072457 | -0.045015 | 0.029896 | -0.019323 |

coupled NLS equations. Our results for the nontrivial configurations at  $\epsilon = 1$  are summarized in Table 1.

Though computations for two and three modes suggest that an alternating configuration of  $\pm 1$ 's can always be successfully continued to  $\epsilon = 1$ , this is not the case, as the following computations demonstrate. We first make the additional simplification, observing that the values of  $b_j$  in Table 1 are close to  $j^2/3$ . This motivates fixing them as such and solving the problem only for the amplitudes,  $\mathbf{a}$ . Thus, we solve

$$(4.8) \quad \nabla_{\mathbf{a}} H_{\text{Gauss}}^N(\mathbf{a}, \mathbf{b}_*, \epsilon) = 0,$$

where  $\mathbf{b}_*$  is given by (4.7). The results of our computations with these fixed variances are given in Table 2. Continuation from the alternating branch  $\boldsymbol{\sigma} = (1, -1), (1, -1, 1), \dots$  is successful until  $N = 4$ . The alternating branch cannot be continued to  $\epsilon = 1$  for five and six modes, though there are other initial states that can be continued to  $\epsilon = 1$ , with sign alternations at  $\epsilon = 1$ ; see Table 2.

Although these results were initially computed using a naive continuation algorithm in MATLAB, solving with a given value of  $\epsilon$  and using that solution as the initial guess for a larger value of  $\epsilon$ , they were confirmed by our computations using AUTO [7, 8].

Though the starting branch may not have an alternating sign structure, sign alternating solutions may still be found at  $\epsilon = 1$ . This makes it challenging to perform numerical continuation with these branches if we no longer assume the variances to be fixed. For a system of five modes,  $a_7$  is positive for small values of  $\epsilon$  and negative for  $\epsilon = 1$ ; hence it must change sign for an  $\epsilon \in (0, 1)$ . When it crosses zero, the variance becomes ill-defined introducing numerical difficulties. On the other hand, if we iterate the system (4.5) near the solution of (4.8) for  $\epsilon = 1$ , the convergence is usually achieved with few iterations.

**4.3. Tails of the variational solutions.** Although we are able to construct a sequence of trial function approximations with Gaussian ansatz, it is not yet clear if such solutions should

exist in space  $X^s$  for  $s > 1$  or at least have finite power ( $L^2$ ) in the limit  $N \rightarrow \infty$ . Indeed, the solution  $(\mathbf{a}_*, \mathbf{b}_*)$  given by (4.4) for  $\epsilon = 0$  with all  $a_p \neq 0$  has infinite power, since

$$\sqrt{\frac{2}{\pi}} \int_{\mathbb{R}} |a_p \exp(-b_p \zeta^2)|^2 d\zeta = \left(\frac{2}{3}\right)^{3/2} \frac{1}{|p|\Gamma^2}$$

and  $\sum_{p \in \mathbb{Z}_{\text{odd}}} \frac{1}{|p|} = \infty$ . However, the results of Table 2 show that at  $\epsilon = 1$ , the sign alternating amplitudes  $\{a_p\}_{p \in \mathbb{Z}_{\text{odd}}}$  are also decaying in  $p \in \mathbb{Z}_{\text{odd}}$ . We explore whether or not the decay is sufficiently rapid to have finite power and to belong to the energy space, where  $H_{\text{Gauss}}$  is finite. To this end, we employ a more refined trial-function ansatz, allowing for weak decay of  $a_p$ :

$$(4.9) \quad a_p = A(-1)^{(|p|-1)/2} |p|^{-\gamma}, \quad b_p = \frac{p^2}{3}, \quad p \in \mathbb{Z}_{\text{odd}},$$

where  $A$  and  $\gamma$  are unknown parameters to be determined from the Euler–Lagrange equations. If  $\gamma > 0$ , the trial function approximation has both  $H_{\text{Gauss}}$  and  $N_{\text{Gauss}}$  finite.

Substituting (4.9) into (4.2) yields a two-parameter Hamiltonian

$$(4.10) \quad h(\gamma, A) = A^2 f(\gamma) - A^4 \Gamma g(\gamma),$$

where

$$(4.11a) \quad f(\gamma) = \sum_{p \in \mathbb{Z}_{\text{odd}}} \frac{4}{\sqrt{3}} |p|^{-1-2\gamma},$$

$$(4.11b) \quad g(\gamma) = \sum_{p, q \in \mathbb{Z}_{\text{odd}}} \sqrt{3} \frac{p^{-2\gamma} q^{-2\gamma}}{\sqrt{p^2 + q^2}} + \sum_{p, q, r \in \mathbb{Z}_{\text{odd}}} \sqrt{\frac{2}{3}} (-1)^{(|p|+|q|+|r|+|p-q-r|)/2} \frac{|p|^{-\gamma} |q|^{-\gamma} |r|^{-\gamma} |p-q-r|^{-\gamma}}{\sqrt{p^2 + q^2 + r^2 + (p-q-r)^2}}.$$

Solving  $\partial_A h(\gamma, A) = 0$ , we find

$$A^2(\gamma) = \frac{f(\gamma)}{2\Gamma g(\gamma)}.$$

Plugging this back into (4.10), we get

$$(4.12) \quad \tilde{h}(\gamma) = h(\gamma, A(\gamma)) = \frac{f(\gamma)^2}{2\Gamma g(\gamma)} - \frac{f(\gamma)^2}{4\Gamma g(\gamma)} = \frac{1}{4\Gamma} \frac{f(\gamma)^2}{g(\gamma)}.$$

Truncating this approximation to  $N$  modes,  $\tilde{h}^N(\gamma)$ , we are able to identify a sequence of critical points, suggesting convergence as  $N \rightarrow \infty$  and the existence of a critical point in the primitive functional (4.12). A few of these approximations are plotted in Figure 3 with  $\Gamma = 1$ . All of the computed  $\tilde{h}^N(\gamma)$ 's have the property that

$$(4.13) \quad \lim_{\gamma \rightarrow \infty} \tilde{h}^N(\gamma) = \tilde{h}^1(\gamma) = \frac{8}{9} \sqrt{\frac{2}{3}}.$$

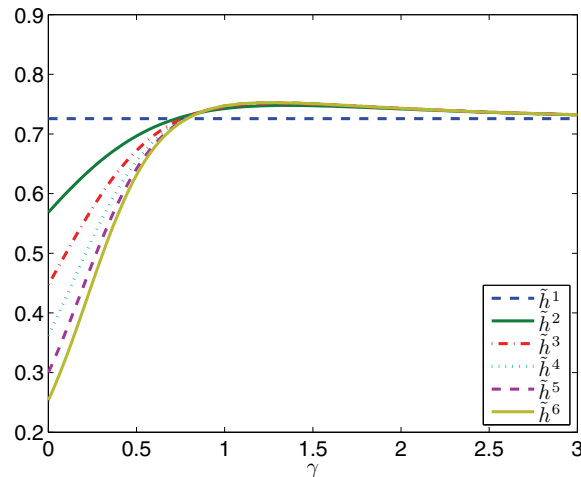


**Figure 3.** Two-parameter approximation (4.9) of  $H_{\text{Gauss}}$  for different truncations.

**Table 3**

Computed critical values of  $\gamma$  for the curves in Figure 3.

| No. of modes | $\gamma_*$ | $\Delta\gamma_*$ |
|--------------|------------|------------------|
| 2            | 1.35511    | -                |
| 3            | 1.30184    | 0.05327          |
| 4            | 1.28176    | 0.02008          |
| 5            | 1.27208    | 0.00968          |
| 6            | 1.26672    | 0.00536          |

The critical values of  $\gamma$ ,  $\gamma_*$  are given in Table 3. These appear to converge to a value of  $\gamma$  near  $\gamma = 1.26$  indicating that the corresponding variational approximations belong to the energy space of the coupled NLS equations. Moreover, since

$$\|U\|_{X^s} \sim \sum_{p \in \mathbb{Z}_{\text{odd}}} |p|^{2s-1} |a_p|^2 \sim \sum_{p \in \mathbb{Z}_{\text{odd}}} |p|^{2s-1-2\gamma}$$

and  $\gamma \approx 1.26$ , the corresponding variational approximations belong to the space  $X^s$  for  $s < \gamma$ . Therefore, the results of Theorems 3.1 and 3.2 can be used in the nonempty interval for the values of  $s \in (1, \gamma)$ . As it appears that  $\gamma$  is strictly greater than one as the number of modes increases, a solution of infinitely many modes might be more regular than  $H^1$ .

The sign alternating structure of the ansatz (4.9) is fundamental for the existence of the critical point of  $h(\gamma, A)$ . For the variational ansatz,

$$(4.14) \quad a_p = A |p|^{-\gamma}, \quad b_p = \frac{p^2}{3}, \quad p \in \mathbb{Z}_{\text{odd}},$$

we can redo the computations to obtain Figure 4. No critical point of  $h(\gamma, A)$  exists for the sign-definite variational approximation (4.14).

**5. Numerically computed gap solitons.** Motivated by our observations from the results of our trial function approximations, we solve the xNLS (3.34) directly to explore the existence

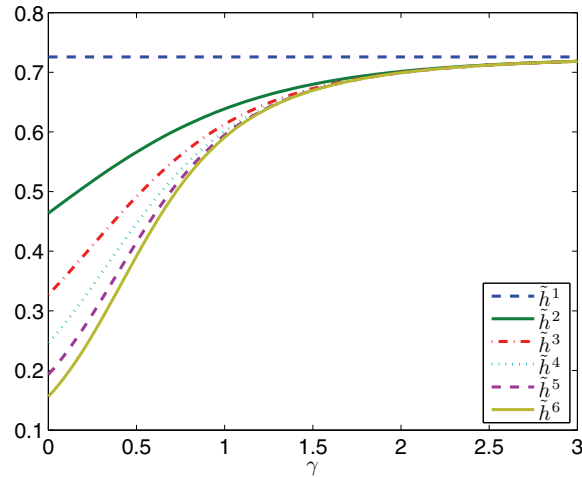


**Figure 4.** Two-parameter approximation (4.14) of  $H_{\text{GAUSS}}$  for different truncations.

of gap solitons. We note that in [22], the authors explored the related problem of solitons of xNLCME truncated to two modes.

**5.1. Computation of gap solitons.** We numerically solve equations (3.34) by continuation. Our starting point is the exact solution at  $\epsilon = 0$ ,

$$U_p(\zeta; \epsilon = 0) = \frac{\sigma_p}{\sqrt{3}\Gamma} \text{sech}(p\zeta),$$

where  $\sigma$  is a branch found in section 4.2 that led to a nontrivial solution at  $\epsilon = 1$ . Incrementing the value of  $\epsilon$ , we solve the system (3.34) using the MATLAB `bvp5c` algorithm with absolute tolerance  $10^{-4}$  and relative tolerance  $10^{-8}$  on the domain  $[0, 25]$ . `bvp5c` is a nonlinear finite difference algorithm for two-point boundary-value problems discussed in [20]. We use the even symmetry of the solutions to impose the boundary condition  $U_p'(0) = 0$  and the artificial boundary condition

$$U_p'(\zeta_{\max}) + pU_p(\zeta_{\max}) = 0$$

to approximate the correct exponential decay.

The results for systems of up to six coupled NLS equations at  $\epsilon = 1$  are displayed in Figure 5. As we can see, the amplitude decays in  $p$ . Moreover, as the number of modes is increased, each mode's profile appears to stabilize to a limiting profile. We conjecture that this profile persists as additional modes are included. Alternatively, the solution can be expressed as  $U(\zeta, \theta)$  by combining the Fourier modes. The resulting solution surface of the integro-differential equation (3.20) appears in Figure 6. The inclusion of additional harmonics induces a more ornate structure near the extrema.

Although we have computed these finite truncation solutions, we ask again whether the corresponding solutions have finite power. For our computed solutions, we find that the power,  $N_{\text{xNLS}}$ , appears to converge, and most of the power remains in the first mode. The data is given in Table 4.

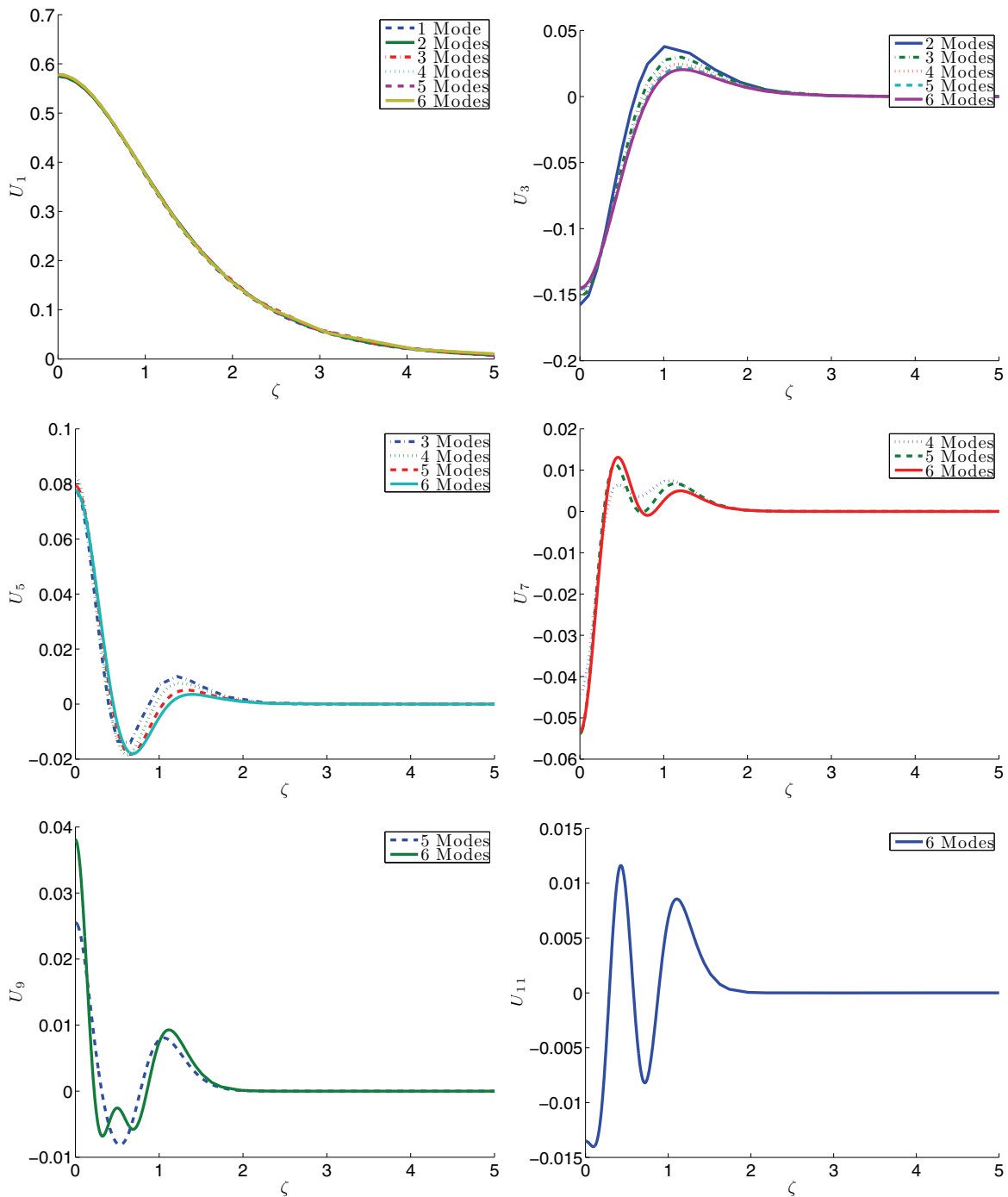
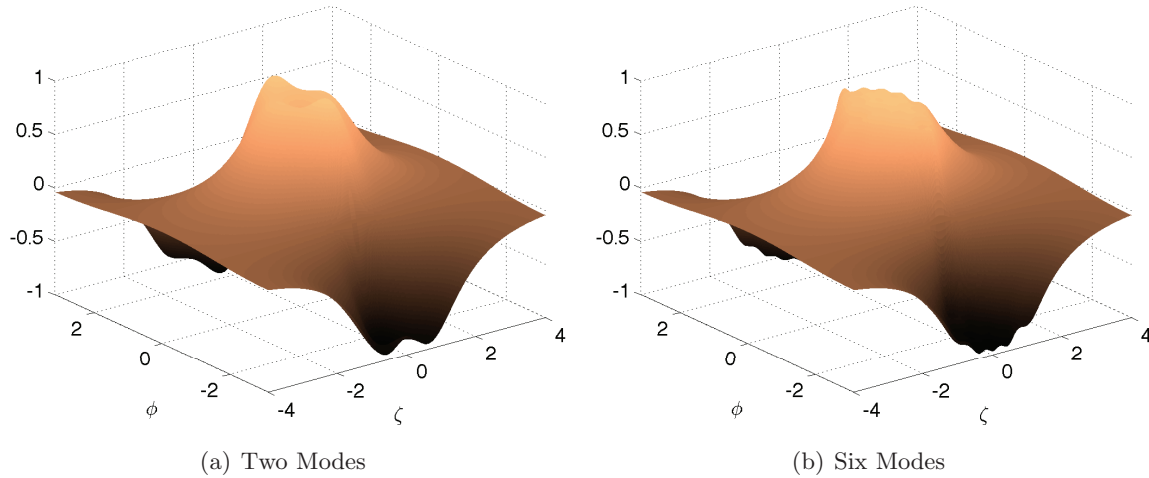


Figure 5. Soliton profiles for the coupled NLS equations (3.19).





**Figure 6.** The solution surface of the integro-differential equation (3.20) generated by the truncated coupled NLS soliton in Figure 5.

**Table 4**

Computed powers for the soliton profiles appearing in Figure 5.

| No. of modes | $\ U_1\ _{L^2}^2$ | $\frac{1}{2}N_{\text{xNLS}}$ | $\frac{1}{2}N_{\text{xNLS}} - \ U_1\ _{L^2}^2$ |
|--------------|-------------------|------------------------------|--|
| 1            | 0.66667           | 0.66667                      | 0  |
| 2            | 0.66982           | 0.68582                      | 0.016000                                       |
| 3            | 0.67147           | 0.68929                      | 0.017825                                       |
| 4            | 0.67211           | 0.69031                      | 0.018201                                       |
| 5            | 0.67226           | 0.69070                      | 0.018441                                       |
| 6            | 0.67236           | 0.69088                      | 0.018523                                       |

**5.2. Gap solitons in time-dependent simulations.** Small amplitude gap soliton solutions of the coupled NLS equation (3.19) can be used as initial conditions in the coupled mode equations (1.10) to assess their stability and robustness. Once the solution  $\{U_p(\zeta)\}_{p \in \mathbb{Z}_{\text{odd}}}$  is computed, the initial conditions for the time-dependent simulation are given by

$$(5.1) \quad E_p^+(Z, 0) = \mu U_p(\mu Z), \quad E_p^-(Z, 0) = -\mu U_p(\mu Z), \quad p \in \mathbb{Z}_{\text{odd}},$$

with even modes set to zero. By Theorem 3.1, the small amplitude approximation is accurate only up to  $\mathcal{O}(\mu^2)$ . We view this small error as an initial data perturbation in the time evolution of the coupled mode equations (1.10). In this way, our numerical results address simultaneously the existence of stationary solutions to xNLCME, their differences from the stationary solutions of xNLS, and the stability of these stationary solutions.

We present the results of two- and four-mode systems. In each case, we truncate both the system of coupled NLS equations (3.19) and the coupled mode equations (1.10) at the same number of resolved modes. In our simulations, we take as our constants

$$v_g = 1, \quad N_0 = 0, \quad N_{2p} = 1, \quad \Gamma = 1.$$

The simulations were performed with the indicated number of grid points using a pseudo-spectral discretization and fourth order Runge–Kutta time stepping. For both the two- and four-mode simulations, the initial conditions (5.1) were computed with greater precision than in the previous section; the absolute tolerance was  $10^{-7}$ , the relative tolerance was  $10^{-9}$ , and the domain was  $[0, 35]$ .

In Figures 7 and 8, we plot the normalized time-space surfaces of  $|E_p^+|$  from our simulations of the first four odd modes. For both values of  $\mu$ , the solution is persistent, but the oscillations are greater for the larger value of  $\mu$ , and there is some decoherence near the peak. With the smaller value of  $\mu$ , there is far less distortion. Additional details of the dynamics are available online in the following animations:

*Two-mode truncation.* The following simulations were computed with 1024 grid points. The  $\mu = 0.4$  simulations were computed on the domain  $[-50, 50]$ , the  $\mu = 0.2$  simulations were computed on the domain  $[-100, 100]$ , and the  $\mu = 0.1$  simulations were computed on the domain  $[-200, 200]$ .

1. 83789\_01.mov [[local/web](#) 4.71MB],
2. 83789\_02.mov [[local/web](#) 1.58MB].

*Four-mode truncation.* The following simulations were computed with 2048 grid points. The  $\mu = 0.4$  simulations were computed on the domain  $[-50, 50]$ , the  $\mu = 0.2$  simulations were computed on the domain  $[-100, 100]$ , and the  $\mu = 0.1$  simulations were computed on the domain  $[-200, 200]$ .

1. 83789\_03.mov [[local/web](#) 4.72MB],
2. 83789\_04.mov [[local/web](#) 4.48MB],
3. 83789\_05.mov [[local/web](#) 4.50MB],
4. 83789\_06.mov [[local/web](#) 4.58MB].

As one would expect, there is better agreement between the approximate small amplitude soliton and the time-dependent simulation as  $\mu \rightarrow 0$ . However, for all values of  $\mu$  presented, there is a persistence of the localization, even if there is distortion of some of the fine structure in the higher harmonics. All of this suggests that the gap solutions are robust.

Many other experiments are possible: simulating with more modes, simulating with larger values of  $\mu$ , and seeding the initial conditions of a smaller system into a larger system. In the previous work [21], the exact gap soliton (3.10) was used as an initial condition for successively larger truncations of the extended coupled mode system (1.10).

**6. Open problems.** We conclude this work with a discussion of open problems concerning the existence of nontrivial localized solutions of xNLCME and xNLS arising for the case of a refractive index composed of an infinite array of Dirac delta functions. The challenges include the following:

1. Prove the existence of a nontrivial critical point to  $h$  (4.10), the single parameter trial function approximation.
2. Prove the existence of a nontrivial solution to  $H_{\text{Gauss}}$  (4.2), the Gaussian trial function approximation.
3. Prove the existence of a nontrivial solution to the coupled NLS equations (3.19).
4. Prove the existence of a nontrivial solution to the coupled mode equations (3.3).

By “nontrivial,” we mean a solution in which all modes are active and nonzero. It would also be of interest to obtain proofs of existence for arbitrarily large finite truncations of these

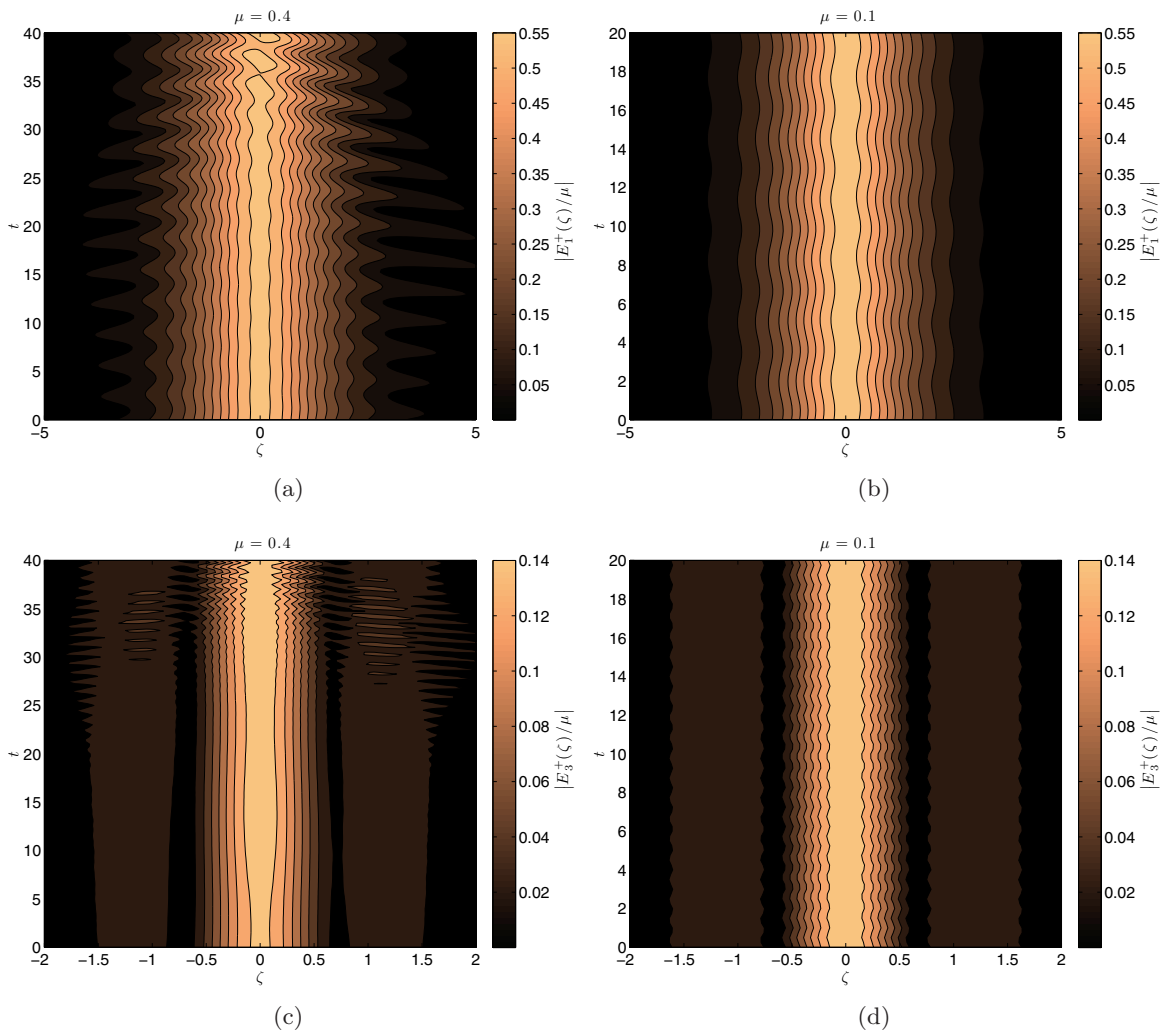


**Figure 7.** Surfaces generated from simulations of the coupled mode system (1.10) truncated to four modes with initial data (5.1). The  $\mu = 0.4$  simulations were computed on the domain  $[-50, 50]$ , and the  $\mu = 0.1$  simulations were computed on the domain  $[-200, 200]$ . In both cases, there were 2048 grid points.

problems. Intimately connected with the last two challenges is the question of appropriate function spaces. As discussed in section 4.3, our variational approximations live in the function space  $X^s$  for  $1 < s < \gamma \approx 1.26$  for which our Theorems 3.1 and 3.2 are stated. The upper value on  $s$  that ensures that the interval is nonempty is only approximated numerically from the “rough” variational approximation. Of course, it is also possible that such solutions may not exist. A counterexample would also be of interest.

Modeling the nonlinear Maxwell equation with refractive index given by a periodic sequence of Dirac delta-functions is a challenging problem both analytically and numerically. Results of our work give a starting point for further exploration of this system and the evolution of its localized excitations. The question of localized solutions for xNLCME for less restrictive, and more physical, refractive indices is also of great interest.

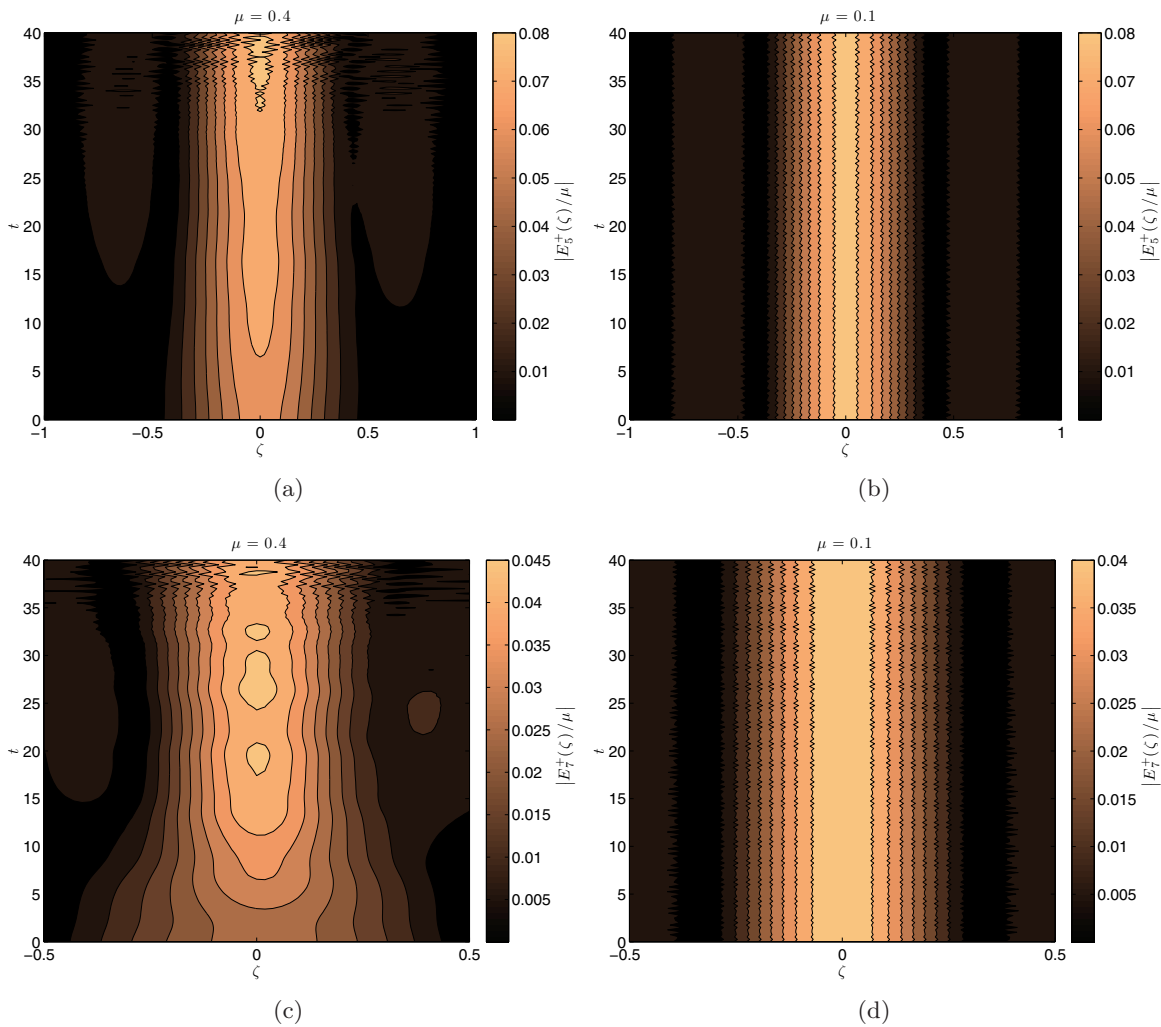


Figure 8. Continuation of Figure 7.

## REFERENCES

- [1] A. B. ACEVES AND S. WABNITZ, *Self-induced transparency solitons in nonlinear refractive periodic media*, Phys. Lett. A, 141 (1989), pp. 37–42.
- [2] D. AGUEEV AND D. PELINOVSKY, *Modeling of wave resonances in low-contrast photonic crystals*, SIAM J. Appl. Math., 65 (2005), pp. 1101–1129.
- [3] R. W. BOYD, *Nonlinear Optics*, Elsevier/Academic Press, Amsterdam, 2008.
- [4] D. N. CHRISTODOULIDES AND R. I. JOSEPH, *Slow Bragg solitons in nonlinear periodic structures*, Phys. Rev. Lett., 62 (1989), pp. 1746–1749.
- [5] M. CHUGUNOVA AND D. PELINOVSKY, *Block-diagonalization of the symmetric first-order coupled-mode system*, SIAM J. Appl. Dyn. Syst., 5 (2006), pp. 66–83.
- [6] C. M. DE STERKE AND J. E. SIPE, *Gap solitons*, Progr. Opt., 33 (1994), pp. 203–260.
- [7] E. DOEDEL, *AUTO: A program for the automatic bifurcation analysis of autonomous systems*, Congr. Numer., 30 (1981), pp. 265–284.

- [8] E. J. DOEDEL, A. R. CHAMPNEYS, F. DERCOLE, T. FAIRGRIEVE, Y. KUZNETSOV, B. OLDEMAN, R. PAF-FENROTH, B. SANDSTEDE, X. WANG, AND C. ZHANG, *AUTO-07P*, <http://indy.cs.concordia.ca/auto/> (2007).
- [9] T. DOHNAL, D. PELINOVSKY, AND G. SCHNEIDER, *Coupled-mode equations and gap solitons in a two-dimensional nonlinear elliptic problem with a separable periodic potential*, *J. Nonlinear Sci.*, 19 (2009), pp. 95–131.
- [10] T. DOHNAL AND H. UECKER, *Coupled-mode equations and gap solitons for the 2D Gross–Pitaevskii equation with a non-separable periodic potential*, *Phys. D*, 238 (2009), pp. 860–879.
- [11] B. J. EGGLETON, C. M. DE STERKE, AND R. E. SLUSHER, *Nonlinear propagation in superstructure Bragg gratings*, *Opt. Lett.*, 21 (1996), pp. 1223–1225.
- [12] B. EGGLETON AND R. E. SLUSHER, EDS., *Nonlinear Photonic Crystals*, Springer, New York, 2003.
- [13] R. H. GOODMAN, R. E. SLUSHER, AND M. I. WEINSTEIN, *Stopping light on a defect*, *J. Opt. Soc. of Amer. B*, 19 (2002), pp. 1635–1652.
- [14] R. H. GOODMAN, M. I. WEINSTEIN, AND P. J. HOLMES, *Nonlinear propagation of light in one-dimensional periodic structures*, *J. Nonlinear Sci.*, 11 (2001), pp. 123–168.
- [15] D. PELINOVSKY AND G. SCHNEIDER, *Justification of the coupled-mode approximation for a nonlinear elliptic problem with a periodic potential*, *Appl. Anal.*, 86 (2007), pp. 1017–1036.
- [16] D. PELINOVSKY AND G. SCHNEIDER, *Moving gap solitons in periodic potentials*, *Math. Methods Appl. Sci.*, 31 (2008), pp. 1739–1760.
- [17] J. K. RANKA, R. S. WINDELER, AND A. J. STENTZ, *Visible continuum generation in air-silica microstructure optical fibers with anomalous dispersion at 800 nm*, *Opt. Lett.*, 25 (2000), pp. 25–27.
- [18] G. SCHNEIDER AND H. UECKER, *Nonlinear coupled mode dynamics in hyperbolic and parabolic periodically structured spatially extended systems*, *Asymptot. Anal.*, 28 (2001), pp. 163–180.
- [19] G. SCHNEIDER AND H. UECKER, *Existence and stability of modulating pulse solutions in Maxwell’s equations describing nonlinear optics*, *Z. Angew. Math. Phys.*, 54 (2003), pp. 677–712.
- [20] L. F. SHAMPINE, I. GLADWELL, AND S. THOMPSON, *Solving ODEs with MATLAB*, Cambridge University Press, Cambridge, UK, 2003.
- [21] G. SIMPSON AND M. I. WEINSTEIN, *Coherent structures and carrier shocks in the nonlinear Maxwell equations*, *Multiscale Model. Simul.*, 9 (2011), pp. 955–990.
- [22] R. S. TASGAL, Y. B. BAND, AND B. A. MALOMED, *Gap solitons in a medium with third-harmonic generation*, *Phys. Rev. E* (3), 72 (2005), 016624.